RSC Advances

REVIEW

View Article Online
View Journal | View Issue

Cite this: *RSC Adv.*, 2024, **14**, 25516

Conducting polymer functionalization in search of advanced materials in ionometry: ion-selective electrodes and optodes

D. Yureka Imali, * E. Chavin J. Perera, * M. N. Kaumal and Dhammike P. Dissanayake

Functionalized conducting polymers (FCPs) have recently garnered attention as ion-selective sensor materials, surpassing their intrinsic counterparts due to synergistic effects that lead to enhanced electrochemical and analytical parameters. Following a brief introduction of the fundamental concepts, this article provides a comprehensive review of the recent developments in the application of FCPs in ion-selective electrodes (ISEs) and ion-selective optodes (ISOs), particularly as ion-to-electron transducers, optical transducers, and ion-selective membranes. Utilizing FCPs in these devices offers a promising avenue for detecting and measuring ions in various applications, regardless of the sample nature and composition. Research has focused on functionalizing different conducting polymers, such as polyaniline and polypyrrole, through strategies such as doping and derivatization to alter their hydrophobicity, conductance, redox capacitance, surface area, pH sensitivity, gas and light sensitivity, *etc.* These modifications aim to enhance performance outcomes, including potential stability/emission signal stability, reproducibility and low detection limits. The advancements have led to the transition of ISEs from conventional zero-current potentiometric ion sensing to innovative current-triggered sensing approaches, enabling calibration-free applications and emerging concepts such as opto-electro dual sensing systems. The intrinsic pH cross-response and instability of the optical signal of ISOs have been overcome through the novel optical signal transduction mechanisms facilitated by FCPs. In this review, the characteristics of materials, functionalization approaches, particular implementation strategies, specific performance outcomes and challenges faced are discussed. Consolidating dispersed information in the field, the in-depth analysis presented here is poised to drive further innovations by broadening the scope of ion-selective sensors in real-world scenarios.

Received 7th April 2024
Accepted 1st August 2024

DOI: 10.1039/d4ra02615b

rsc.li/rsc-advances

1. Introduction

Over the years, there has been a growing interest in the area of "ionometry", which involves using ion-selective sensors (ISSs): ion-selective electrodes (ISEs) and ion-selective optodes (ISOs) for qualitative and quantitative analytical methods. The significance of the practical applicability of "ionometry" drives the impetus for various enhancements in ISEs[1] and ISOs. Numerous ISEs/ISOs have been created for the direct detection of more than 60 inorganic, organic, and biological ions. Additionally, they can indirectly detect various gases, neutral solutes, chemical/biochemical reactions, and bio-recognition events.[2–4] Ions are found extensively in nature and their presence, as well as their concentration levels, play a crucial role in driving mechanisms and processes.[5] Detecting trace amounts of ions is difficult,[6] and ISEs and ISOs are commonly employed for this task.[7–9] Over the past few decades these techniques have emerged as a promising platform for ion sensing.[10–13] ISEs/ISOs have replaced conventional instrumental methods in ion measurement,[2] which involve complex instrumentation and elaborate sample preparation, making *in vivo*, *in situ*, and real-time measurements challenging.[14] These methods include atomic spectroscopy,[2,15,16] ion chromatography,[17] electrophoresis,[18] induction-coupled plasma mass spectroscopy,[19] *etc.* Using ISSs has now become standard practice.[2] Ionophore-based electrochemical and optical sensors enable accurate tracking of changes at crucial analyte concentrations.[7–9] However, there are significant differences between optical and electrochemical devices regarding their practical applications, outweighing their commonalities.[9]

Using ISEs is favoured over other techniques as they are non-destructive and a passive analytical method that converts the activity of primary ions into electrical potential without requiring further stimulation.[6] The cellular functions of the body are regulated by particular ion concentrations.[5] ISEs are employed in the clinical laboratory and point-of-care analysers to determine essential analytes critical for making quick

Department of Chemistry, University of Colombo, Colombo 03, Sri Lanka. E-mail: yurekauoc@gmail.com; chavinperera@gmail.com

decisions about patient care.[20–24] These analytes include Na^+, K^+, Cl^-, Ca^{2+}, Mg^{2+}, and Li^+.[20,21] Plant growth is facilitated by the available micronutrient ions in soil and water. Therefore, ISEs are utilized in agriculture to mediate plant growth and as well as in industrial analyses and process control.[5,25–28] ISEs are indispensable within electrochemical sensors[1] and researchers are particularly interested in using ISEs as they offer several benefits compared to other analytical techniques.[29] These are ease of fabrication, fast response time, high selectivity towards a specific ion, wide linear range, reproducibility, potential for miniaturization,[30] low-cost, low energy consumption,[31] small in size and portable.[32] They enable the direct measurement of crucial ions, even in complex matrices[33–35] like whole blood, without requiring any sample pretreatment.[34,35] There are two types of ISEs. These are ISEs with an internal filling solution and solid-state ISEs (SS-ISEs) without internal filling solutions. Among these two types, SS-ISEs are durable, flexible, maintenance-free, robust, reliable, and portable ion sensors that provide easy miniaturizing capability.[30,32,36,37] They are widely utilized in various fields, including medicine, veterinary science, water treatment, food control, process control, environmental and pollution monitoring, security, *etc.* and employed as a replacement for conventional ISEs that utilize liquid inner contacts.[38]

The ISOs are a specific type of optical chemical sensor.[39] They were originated from polymeric membrane ISEs[40] and regarded as the counterpart of ISEs.[41–43] Their appeal lies in the sensor specificity achieved by directly adopting selective ionophores from ISE counterparts.[40] Their primary advantage stems from the ability to selectively detect ions through the precise binding between an ionophore and the analyte ion during optical chemical sensing.[39] In this scenario, the highly selective neutral ionophores that have been developed for polymeric membrane ISEs can be directly used without requiring any chemical modifications. This aspect has played a significant role in the progress of this methodology alongside the advancement of polymeric membrane ISEs.[39] Moreover, these are versatile devices well-suited for a wide range of applications within diverse areas including medical, environmental, *etc.*[44]

ISSs are well-established analytical tools used in both electrochemical and optical sensing. Currently, the focus in the field of ISSs lies strongly on achieving high stability and versatility. This enables their application across various analytical scenarios, irrespective of the chosen operational mode.[9] The use of conducting polymers (CPs) appears to be particularly beneficial in achieving these objectives.[45] The intrinsic ionic and/or redox sensitivity of the CPs makes them highly useful in a variety of sensor technologies. The use of CPs in sensors provides the opportunity for simplification and integration.[45] CPs are extensively utilized in sensing systems as both transducers and sensing layers, capitalizing on their exceptional electrochemical and optical characteristics.[46] The utilization of CPs in all-solid-state ISEs (ASS-ISEs) is varied, owing to their applicability as materials for ion-to-electron transducers and ion-selective membranes (ISMs). In ISOs, primarily CPs are used as optical transducers.

CPs offer numerous advantages including lightweight design, ease of processing, corrosion resistance, affordability, and exceptional electrical, mechanical, and optical properties.[47,48] CPs such as polypyrrole (PPy), polyaniline (PANI), poly(3-octylthiophene-2,5-diyl) (POT), and poly(3,4-ethylenedioxythiophene) (PEDOT) have been garnering attention due to their fascinating electrical conductivity, electroactivity, and potential use in advanced sensor technology.[49] However, constraints exist with pristine CPs due to inherent limitations. The primary needs of sensors, such as the ability to selectively detect a specific analyte in a complex environment, are challenging to fulfil using pristine CPs alone. The limitations in pristine CPs, as well as challenges in their processability, underscore the requirement for creating functionalized conducting polymers (FCPs). Therefore, the current emphasis is on FCPs. This can be achieved through strategic structural adjustments to the as-synthesized CPs or by incorporating components that alter their functional properties.[50] Different functionalization approaches can be identified, leading to several categories of FCPs used in ISS material preparation, including substituted or derivatized FCPs, nanostructured FCPs, and multicomponent FCPs. Substituted or derivatized FCPs can be prepared through several methods. One approach is the copolymerization of functional group substituted monomers with unsubstituted monomers using oxidative chemical/electrochemical polymerization methods. Another technique is grafting chains of CPs onto a preformed polymer, electrode surface, another substrate, or other nanomaterials (*e.g.*: graphene, metal/inorganic nanoparticles, carbon nanotubes, other polymer nanostructures, *etc.*) through chemical linkages employing preparation methods such as radiation polymerization ("grafting from" or "grafting to" methods). Further, physical adsorption and entrapment of functional group-containing compounds onto the CP, as well as the incorporation of dopant ions (external doping or self-doping) can be employed. In these methods, various substituents can be introduced along the CP backbone, either on the aromatic or heterocyclic ring or on the heteroatom in the main chain of the parent CP, to achieve the desired characteristics.[50] To develop nanostructured FCPs, integrating nanostructured materials like nanowires or nanotubes into CPs or pristine nanostructured CPs can be employed. This type of FCP can be achieved through preparation methods including the hard/soft template-mediated oxidative chemical/electrochemical polymerization method, template-less method, lithographical attachment on substrates, and electrochemical nanostructuring method.[50] The multicomponent FCPs are developed by combining two or more materials with the CPs. Here, chemical/electrochemical polymerization is employed in the presence of different precursors with multiple steps of inclusion.[50]

Interestingly, FCPs combine the benefits of CPs with other sensing materials like carbonaceous materials, metal oxides, metals, *etc.*[47,48] Due to the synergistic effect,[51] FCPs commonly possess improved mechanical, thermal, electrical, optical, and chemical properties compared to their intrinsic counterparts.[52] Numerous studies have shown that, to enhance the performance of ISSs, exploiting the benefits of FCPs is a promising

approach than utilizing their intrinsic counterparts.[51] Moreover, the distinctive properties of FCPs could be strategically leveraged to enhance the precision, responsiveness, and efficiency of sensors, pushing beyond the constraints of current detection methods.[50] The wide range of FCPs and the numerous possibilities for synthesizing and modifying their composition or components contribute to their high popularity among scientists.

This review article focuses mainly on the particular developments that have happened within the past decade. Utilization of FCPs as ion-to-electron transducers, optical transducers, and ISMs is discussed. Strategies for enhancing FCP-based ISEs performances (including stability, reproducibility, and low detection limits), ISOs performance (focusing on emission signal stability), and innovative sensor designs involving FCPs are discussed with specific examples from recent literature. Emphasis is placed on the ion-to-electron transduction mechanism, optical transduction mechanism, and selective sensing through the ISMs with the particular view of better analytical and performance parameters. As well, future perspectives and development trends are introduced. Fig. 1 illustrates the overview of the core content presented in this review. We anticipate that the topics discussed in this article can offer novel insights and practical guidance for advancing ISEs/ISOs. Additionally, we seek to inspire exciting innovations and applications in the continuously evolving field of ISSs by perfectly coordinating with CP functionalization and ultimately reaching the goal of ISSs with better analytical performances.

2. Ion-selective electrodes and their developmental evolution

Since 1950, ISEs have been extensively researched and widely employed across various fields.[49] At the outset, ISEs were devised with an inner electrode, an ISM, and an internal solution positioned between them. This internal solution is in direct contact with the membrane and facilitates the appropriate charge transfer mechanism between the membrane and the discharge electrode.[53] Although they demonstrate very good analytical parameters, the presence of a solution inside the electrode leads to several complications. These are air bubble formation inside the electrode, leakage of the internal solution necessitating regular solution refills, comparatively large electrode size which makes it difficult to store and transport,[53] the inner solution's tendency to evaporate or freeze,[54] and short shelf-lives.[55] Further, the Ag/AgCl internal reference electrode used in many such systems is highly susceptible to oxidation.[56] Hence, extensive research has been conducted on ASS-ISEs[56] as they are versatile, can be utilized at any angle,[57–59] easy to miniaturize,[60] and do not require any refilling.[61]

The coated-wire electrodes (CWEs) were the first concept proposed for internal solution-free sensors.[62] The development of CWEs is considered the pivotal milestone in the evolution of SS-ISEs that consisted of a very simple design.[32] That is a conductor like platinum wire or graphite rod coated with a thin polymeric film containing electroactive materials.[56,63,64] The long-term stability of the electrode potential is highly

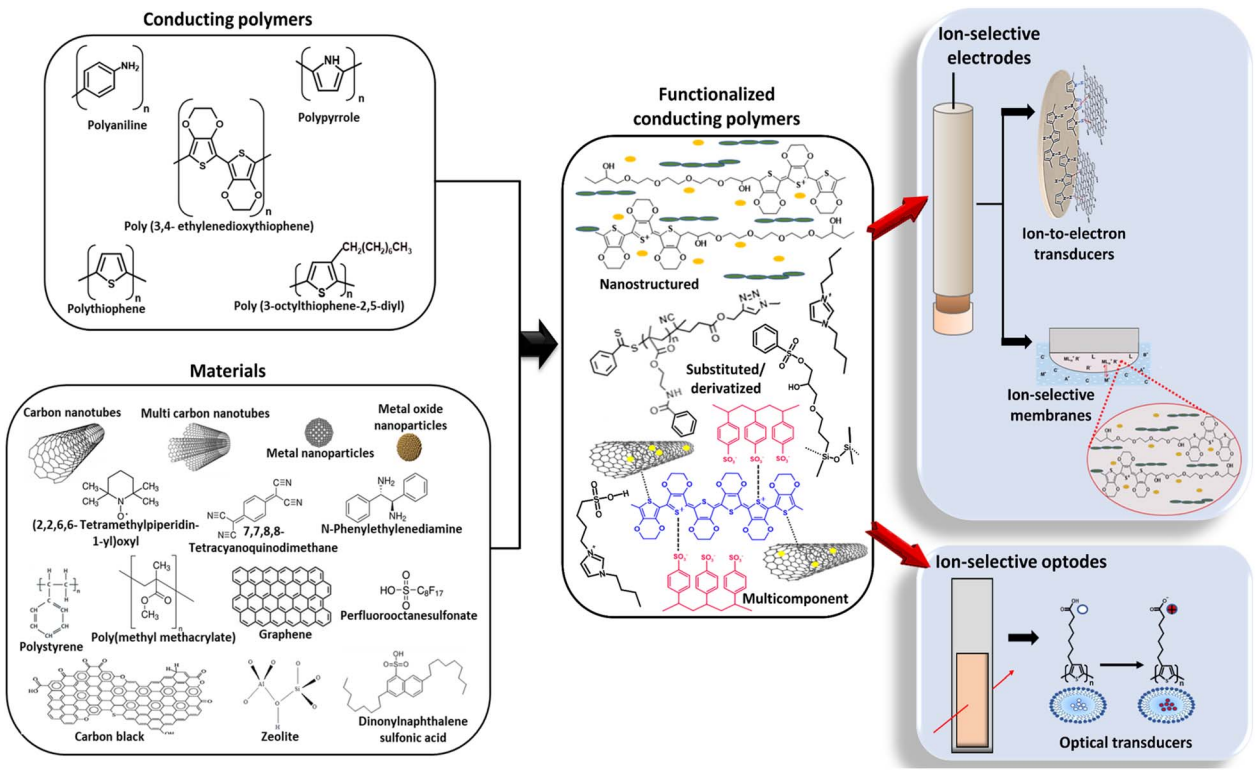

Fig. 1 Schematic illustration summarizing the scope of this review.

significant when ISEs are used in practical settings.[54] However, potential instability is a drawback of these electrodes due to the direct contact between two substances with dissimilar conductivities. This results in a blocked interface for ion-to-electron transduction between the ISM and the underlying electronic conductor,[32,53,62,65,66] causing strict confinement of ions and electrons to their respective phases.[6]

Bobacka *et al.* studied and compared CWEs with solid-contact ion-selective electrodes (SC-ISEs). SC-ISEs were prepared by coating poly(3-octylthiophene) (POT) as solid contact (SC) material with an ISM and CWEs were prepared by coating the bare substrate with the same ISM. The SC-ISEs showed similar potentiometric slopes, detection limits, and response times to the CWEs. Nevertheless, the SC-ISEs demonstrated greater stability in their electrode potential than the corresponding CWEs.[54] There are advantages of CWEs over conventional ISEs with internal filling solutions. It's possible to manufacture the CWEs in different dimensions and shapes and use them in any spatial orientation. Furthermore, the CWEs can be cost-effective to produce since the substrate doesn't need to be a noble metal.[54] Nonetheless, these electrodes exhibit limited long-term stability[27] unstable and non-reproducible potential response.[67] They are useful in specific applications like chromatographic detectors or flow-injection analysis.[27] The potential measurements in such sensors can be influenced by the emergence of an oxygen half-cell or the existence of a slim layer of water between the ISM phase and the contact.[62] As a solution for this and enhancing the potential stability, various transducer layers which also has some shortcomings, such as Ag/AgCl, redox polymers, self-assembled monolayers, and hydrogels, have been suggested. Among these transducers, the hydrogel contact appears to be the most commonly used.[62] Using a hydrogel matrix offers a decent approach as it maintains a precise inner boundary potential similar to liquid contact electrodes and facilitate their mass production through mechanized drop-casting. However, it also introduces several drawbacks in comparison to the benefits. When submerged in an aqueous solution, the hydrogel absorbs water across the membrane, causing it to swell[68,69] and resulting in substantial potential drift. Additionally, inadequate attachment of the ISM to the hydrogel and achieving osmotic balance in the sample adds further complications.[68]

3. Solid-contact ion-selective electrodes

A significant development in the area of SC-ISEs can be observed with the identification of the requirement for well-defined ion-to-electron transduction between two phases that possess different conductance properties.[6] SC-ISEs were developed by incorporating additional material with mixed conductivity as ion-to-electron transducer between substrate electrode and ISM.[53] This resulted in achieving sufficient potential stability[53,70,71] and removing the need for an internal solution.[53] The SC-ISEs are a preferable alternative to traditional ISEs that use an internal filling solution.[72] They have the ability to overcome crucial constraints present in their liquid-contact-based counterparts.[68] The primary concern in SC-ISEs is the reversibility and stability of the ion-to-electron transduction process between the ionically conducting ISM and the electronically conducting substrate.[73] Using an ion-to-electron transducer helped to maintain stable and reversible potential for the sensors, allowed for operation under varying pressure and temperature conditions, and facilitated miniaturization and shape modification.[53] The surface morphology of the SC layer can significantly influence the adhesion between the SC and the ISM.[74] For an effective SC, it is essential to establish a strongly adhesive layer between the electrode support and the membrane material, while avoiding the formation of a thin aqueous layer between them.[75] The characteristics of the transducer material have a notable influence on the parameters of the SC-ISEs.[76] Requirement for a reliable, durable, and miniaturized potentiometric ion sensor is the presence of membranes with ion-recognition sites linked by covalent bonds, along with an all-solid-state ion-to-electron transducer.[77] Potentiometric measurements involve monitoring potential values under zero current conditions to determine the concentration of desired components.[69] Fig. 2 illustrates the developmental evolution of ISEs. This field is currently undergoing intensive research. Many approaches involve the use of ISEs and ISMs with a non-zero current pre-treatment or measurement mode.[78,79]

4. Ion-to-electron transducers

4.1 Ion-to-electron transduction mechanism

SC-ISEs are consisted with ISMs immobilized with lipophilic organic anion (ionophore) which selectively binds with the target ion, conductive substrate which acts as an electronic conductor, and an intermediate SC layer which transforms the input ionic signal into a detectable electrical potential signal by acting as an electrochemical signal transducer.[6] The target ion concentration can be detected by connecting the conductive substrate to a reference electrode that is immersed in the same electrolyte.[80] The conversion from ionic to electronic conductivity is enabled by a SC layer that exhibits both ionic and electronic conductivity[36] ensuring stable and reproducible potentials for practical use.[81] This layer is positioned between the internal reference element and the sensing membrane, facilitating the transfer of conductivity.[36] For SC-ISEs to achieve a response that is stable and reliable, the SC must satisfy three fundamental criteria. These include the ability to transition reversibly between ionic conduction in the ISM and electronic conduction, the absence of polarizable interfaces with high exchange current densities, and the prevention of any side reactions within the SC.[26] To ensure the stability and reproducibility of SC-ISEs, it is crucial to establish a well-defined pathway for ion-to-electron transduction due to the different inherent conductive properties of membranes and substrates.[6] As well, this transduction pathway is associated with the presence of either redox capacitance or double-layer capacitance at the ISM-SC interface. The intrinsic properties of the SC functional materials that serve as ion-to-electron transducers dictate

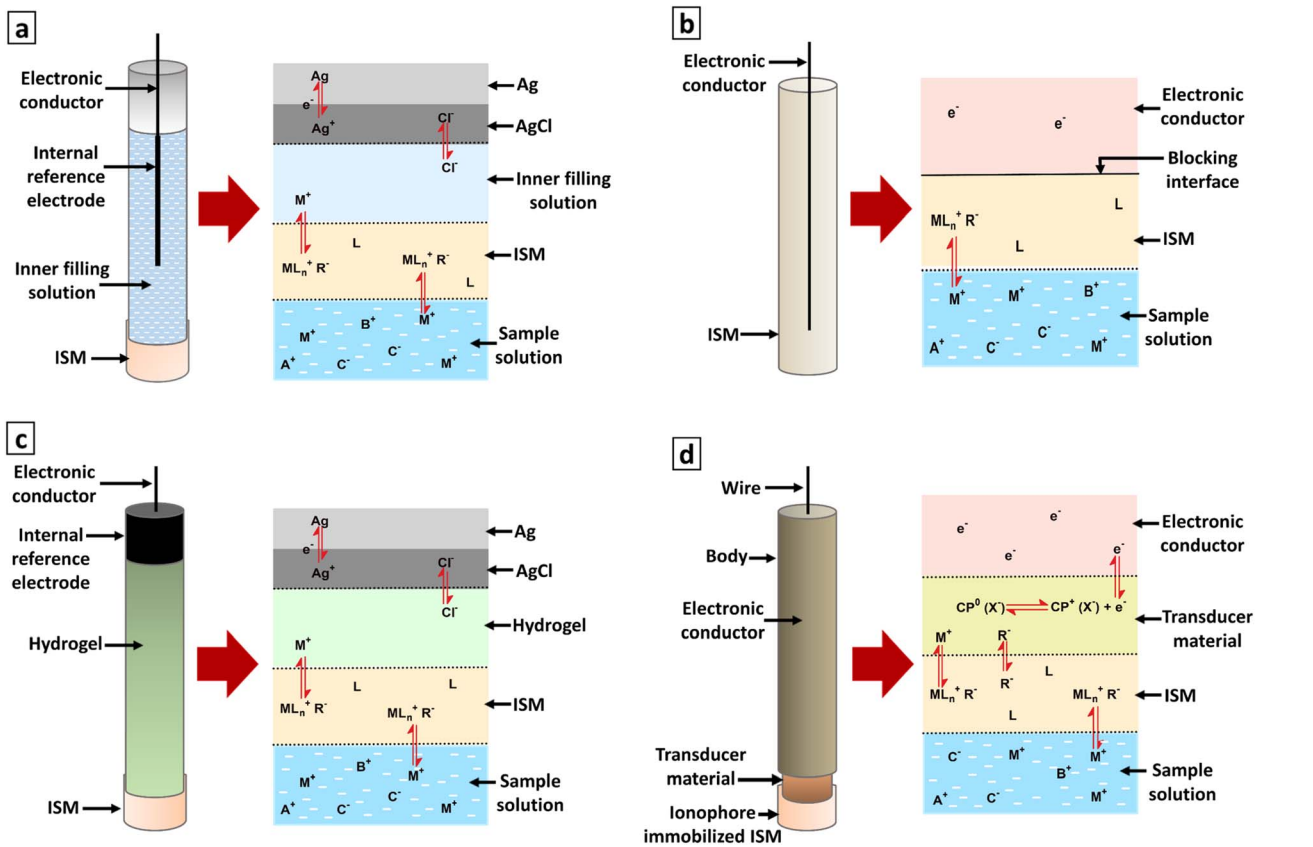

Fig. 2 Progress of development of ISEs from conventional liquid inner filling ISE to SC-ISE through CWE and hydrogel filling ISE, respectively. Structure, schematic representation of all relevant interfaces and sensing mechanism of (a) conventional ISE with inner filling solution, (b) CWE, (c) ISE with hydrogel inner filling and (d) SC-ISE (primary ion (M^+), ionophore (L), ionophore–ion complex (ML_n^+), anionic sites (R^-) and doped ion of CP (X^-)).

the magnitude of this capacitance. Increasing the interfacial capacitance results in improved potential stability.[6]

4.2 Types of materials used as ion-to-electron transducers

In the past decade, advancements in SC-ISE technology have led to the development of different types of SC materials.[82] Many attempts have been made to investigate improved SC materials that possess excellent conductivity, resistance to water absorption, significant capacitance, and exceptional durability.[81] It was proposed that to prevent water layer formation and enhance redox potential accuracy at the membrane/solid support boundary, a lipophilic redox-active layer, like a self-assembled monolayer (SAM), could be introduced between them.[83] The materials used for SC layers in ISEs can be categorized into two main groups: high redox-capacity materials and high double-layer capacity materials.[6,84]

According to the redox capacitance or double-layer capacitance at the ISM-SC interface, SC materials must act as asymmetric capacitors. These transducer elements emit/receive electrons allowing charging or discharging during potentiometric measurements.[6] The interfacial potential can be stabilized by generating above mentioned two types of capacitors; *i.e.* double-layer capacitance and redox capacitance.[6] The double-layer capacitance type ion-to-electron transduction occurs due to the SCs based on functional materials that have a large contact area with the ISM and the conversion of charge carriers based on the presence of large double-layer capacitance formed at the SC-ISM interface. Various micro/nanomaterials with high surface areas have been experimented as ion-to-electron transducers to increase the interfacial contact area between the SC layer and the ISM as they increase the double-layer capacitance.[6,81] Generally, high double-layer capacitance materials include nanostructure noble metals and carbon-based materials such as carbon nanotubes, graphene, *etc.*[6,81]

The electroactive materials that can induce redox capacitance can be employed as SC layers. Mainly these materials include CPs and redox-active self-assembled monolayers, redox couple-doped gold nanostructures, metallic or organic redox couples, ion exchange resins, lipophilic silver complexes, ferrocene, Prussian blue, 7,7,8,8-tetracyanoquinodimethane, tetrathiafulvalene (TTF), *etc.*[6,85] These functional materials undergo a reversible redox reaction during the ion-to-electron transduction process. The target ion reversibly binds to an ionophore at the ISM-solution interface and also these species can reversibly transfer across the SC|ISM interface causing redox reaction in the SC layer.[6] Metal oxides, due to their

nanometric size, display both high redox activity and substantial surface area.[86]

5. Conducting polymer-based ion-to-electron transducers

5.1 Intrinsic CPs as ion-to-electron transducers

CPs which are also referred to as synthetic metals[54] are widely recognized as the preferred materials for SC-ISEs.[81] The use of CPs as a SC layer marked a vital breakthrough in ISE design.[63] These are a special class of polymers that possess unique electronic characteristics attributed to their π-electron backbone.[87] CPs can be classified into two categories; redox polymers and intrinsic electroconductive polymers, based on the movement of electric charges determined by their polymer chemical structure.[88] CPs contain semiconducting molecular architectures and captivating attributes well-suited for sensing applications, which result from electronic conjugation between each recurring unit within them.[50] Exposure of CPs to an analyte triggers various changes, such as solvation effects on the polymer chain, modifications in the conformation of the backbone, and the attraction of dopant counter ions or the transfer of electrons. These changes ultimately result in alterations in electron mobility and the swelling of the polymer matrix, which can be transformed into electrical and/or mechanical signals.[47]

CPs have been studied and are currently being investigated with a particular focus on their use as internal contact materials to stabilize the electrode potential and avoid the use of an inner filling solution.[89,90] In order to attain optimal ion-to-electron transduction and maintain a stable potential, it is typically essential for p-doped CPs with low oxidation potentials, to be in their conducting form.[91] Certain CPs commonly employed as ion-to-electron transducers have been discovered to possess oxidation/reduction characteristics that can trigger ion-transfer processes across the membrane/sample interface.[85] CPs possess the following inherent characteristics, rendering them appropriate for utilization as ion-to-electron transducers in SC-ISEs. CPs can establish an ohmic connection with high-work function materials (*e.g.*, carbon, gold, and platinum). Electrochemical polymerization of a diverse range of monomers allows for the easy electrodeposition of CPs onto electronic conductors. Further, the existence of soluble CPs and their ability to be deposited from solutions. CPs possess both electronic and ionic conductivity, making them electroactive materials capable of converting an ionic signal into an electronic one within a solid-state system.[32]

The ion-to-electron transduction process that happens in electrodes is asymmetric. Therefore, having an intermediate layer with a high redox capacitance is necessary to reduce the polarizability of the SC. The type of SC used in the ISE is crucial in determining the magnitude of this capacitance.[92] The high redox capacitance provided by the CPs as intermediate layers makes them well-suited to serve as ion-to-electron transducers in SC-ISEs.[32,92] The ability of CPs to exhibit high redox capacitance is due to redox buffering capacity resulting from their inherent properties of ionic and electronic conductivities, which can be modified by the doping agents. The ion-to-electron transduction that takes place in the CPs is limited to its surface and determined by the surface reactivity and electrical capacitance.[6] The mobility of ions within the CP and the transfer of ions between the CP and ISM phases significantly impact the interfacial capacitance.[75]

Considering the necessity of transducers with combined ionic and electronic conduction, CPs present a clear advantage.[93] This is because most CPs achieve electronic conductivity by doping with an ionic additive. Consequently, these polymers demonstrate electronic conductivity along the polymer backbone, enabling electron exchange with the electrode through redox reactions. Simultaneously, dopant ions exchange at the interface with the sensing membrane.[84,93] One major benefit of CPs is that they combine electronic and ionic conductivity, allowing for reversible charge transfer across all sensor interfaces.[72]

The CPs that have been most extensively researched for use as SCs are PPy, PANI, POT, and PEDOT,[72,74,94,95] and their derivatives (Fig. 3).[55] These polymers can be deposited onto a substrate using either electropolymerization or drop-casting from a polymer solution. The method of CP-based SC layer formation has an influence on the sensor performances. It has been observed that the stability of SC-ISEs is superior when a solvent-cast POT layer is used compared to ISEs with an electropolymerized layer. This difference in stability is attributed to variations in the formation of a water layer.[93,96] Among these CPs, PANI, PPy, and PEDOT consisted with high stability, conductivity, and redox capacitance. Nonetheless, their electrical activity across a broad range of potentials can cause potential drift as a result of side reactions.[72] POT and PANI were

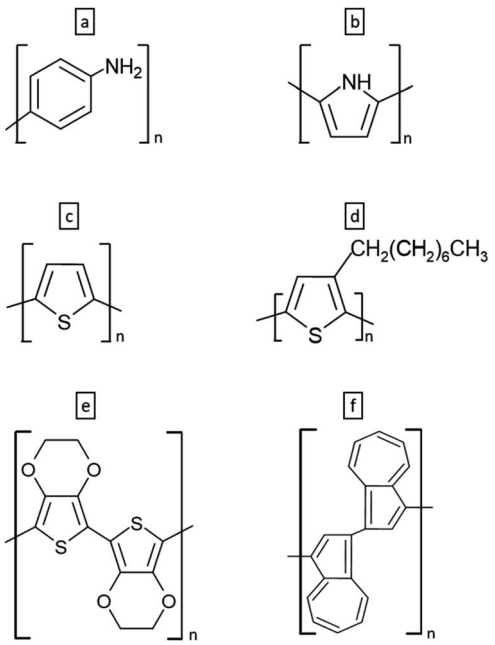

Fig. 3 Commonly employed CPs as SC materials. (a) Polyaniline, (b) polypyrrole, (c) polythiophene, (d) poly(3-octylthiophene-2,5-diyl), (e) poly(3,4-ethylenedioxythiophene) and (f) polyazulene.

also employed as transducers, being directly dissolved within the membrane itself, instead of being positioned as a distinct separate layer between the ISM and the underlying electron conductor.[61,93] This approach resulted in a robust potentiometric response, with no sensitivity to redox-active species in the solution when a low concentration of the CP was present in the membrane.[93,97] Additionally, CPs such as polyazulene (PAz) and ferrocene functionalized poly(vinyl chloride) (PVC), have also been suggested for utilization in SC-ISEs.[81] These polymer-based systems show great promise due to their ability to achieve lower limits of detection (LODs),[98–101] potential for sensor miniaturization,[98] and straightforward construction.[102] As well, utilizing CPs as solid-state transducers is appealing due to their ability to be synthesized in various forms and serve as an additional layer between the sensing membrane and electrode surface.[93] The CP SCs remain stable and chemically unreactive when the ISM comes into contact with various sample solutions.[103]

Therefore, CPs offer desirable features as transducer materials for ISEs,[72] such as the increased signal stability[78,104,105] attributed to the high redox capacitance of the CPs,[92] consistent and reproducible potentials among different sensors. Further, CPs offer the opportunity for tailored analytical performance[72] and have properties that allow for external adjustment and control of the redox state, thereby influencing the potential of the CP,[106,107] which is determined by its ionic content and redox equilibrium.[78] These characteristics can be improved through functionalization and harnessed in novel approaches leading to eliminate calibration requirements upon optimization.[78] These adjustments have been reviewed and discussed in subsequent sections, based on recent literature. However, certain aspects of these systems are not yet fully comprehended at present[98] and CPs possess inherent limitations that are unavoidable and deserve careful attention.

5.2 Shortcomings of intrinsic CP ion-to-electron transducers

CPs offer several benefits and some drawbacks when used as SCs.[25] One of the most commonly experienced issues is the instability of potentiometric measurements using SC-ISEs, which is caused by insufficient adhesion between the layers, resulting in the accumulation of a thin water layer between the ISM and SC (Fig. 4a).[83,108] Establishing an appropriately hydrophobic interface is critical to counteract the formation of the aqueous layer.[91] The "water layer test" is employed to ascertain whether a water layer exists between the ISM and its SC.[83,108] This test involves measuring potential transients that arise from concentration variations in the water layer caused by ion fluxes moving across the ISM into the water layer or from the water layer into the sample.[25] The detection of characteristic potential drift during the water layer test is regarded as evidence of the existence of a water layer (Fig. 4b).[6,25] The unintended water layer, which interacts with membrane-transported species such as CO_2, O_2,[108] primary ions, and interfering ions,[83,96] leads to alterations in the chemistry at the rear of the ISE membrane. This, in turn, negatively affects the sensor's response characteristics,[96,109] including selectivity, potential drift rate often by

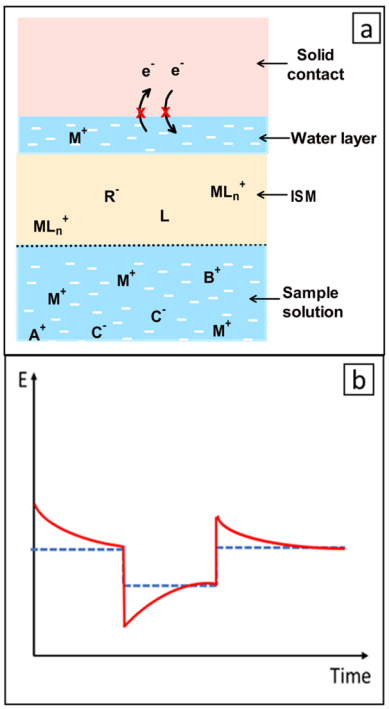

Fig. 4 (a) An unintentionally formed aqueous layer between the ISM and ion-to-electron transducer. (b) Potentiometric water layer test; without water layer (blue dotted line) and with water layer (red line).

a significant magnitude,[96,109] sensitivity to changes in osmolality, and eventually detachment of the membrane from the substrate.[85] This is one of the main factors contributing to potential instability due to subsequent transmembrane flux of primary and interfering ions within the ISM.[51] As well, this hampers the effort to decrease the detection limit of ISEs.[37,109,110] Therefore, the crucial aspect in resolving this issue is the creation of novel materials which are efficient ion-to-electron transducers that possess high hydrophobicity.[85] Therefore, the notable hydrophobic properties of some CPs and their derivatives have been drawn much attention in this context. Besides this, the practical use of electrodes modified with CPs-type membranes is hindered by the unavoidable water layer and oxidation reaction between SC and the ISM, particularly due to dissolved oxygen.[56] Since many CPs are sensitive to O_2, CO_2, pH, or light,[37] there is a potential for undesired electrochemical side reactions that can be triggered by these environmental factors.[81]

CPs typically lack distinct standard redox potentials (E°) and to enable continuous sensing, stabilizing the E° of the SC-ISE is crucial and essential.[111] The inadequate long-term electromotive force (emf) stability may be attributed to the presence of multiple polymer conformations, causing a wide range of redox activity instead of a well-defined redox buffer. Redox-active self-assembled monolayers, controlled by applied current, exhibited sensors with minimal drift but limited redox buffer capacity.[105] E° instability necessitates frequent calibrations to ensure reliable and consistent analytical results. Therefore to maintain accurate and consistent analytical results, ISEs need regular calibration using calibration solutions.[112,113] Consequently,

there is a demand for calibration-free potentiometric sensors to improve their decentralized applications. Active research is underway to address the issue of E° irreproducibility.[105] Additionally, in SC-ISEs, it may seem that there are no transmembrane fluxes since there is no internal electrolyte.[114] However, the internal reference system of a CP-based SC-ISE, can also introduce analyte ions into sample solutions, albeit to a lesser extent compared to ISEs with internal aqueous solutions.[114,115]

Some CPs such as PANI are pH sensitive. The primary drawback for the extended usage of PANI-based SCs is most likely the gradual transformation of its conductive state into a non-conductive form, which typically occurs over several months.[93,103] Another concern involves the unregulated and spontaneous transfer of CP transducer material to the ISM phase, both during the sensor preparation step and the sensor's pre-treatment before use, which can potentially alter the intended sensor performance. Jaworska *et al.* have studied this phenomenon using POT as a model transducer system. Based on the recorded fluorescence microscopic images, a greater concentration of the CP was observed near the interface between the receptor layer and the sample. This phenomenon leads to a spontaneous alteration in the oxidation state of POT, facilitated by anionic lipophilic additives from the ISM acting as dopants. It was found that the presence of the CP within the membrane plays a role, to a certain extent, in influencing the overall response of the sensor.[116]

5.3 FCPs as ion-to-electron transducers

Despite extensive research endeavours, the potential stability of SC-ISEs, particularly those utilizing CP-based transducers, continues to pose an unresolved challenge, impeding their commercialization.[51] Earlier, robust, durable, and miniaturized SC-ISEs with excellent potential stability with potential drift less than *ca.* 0.1 mV h^{-1} were the main targets of researchers. Over time, various demands emerged such as development of calibration-free sensors that could be utilized as single-use and wearable sensors, *etc.*[117] To achieve sustained long-term stability, it is crucial to possess a redox functionality that is exceptionally stable, reversible, immune to light-induced degradation, and resistant to oxidation by molecular oxygen. Additionally, the hydrophobic properties of the SC materials need to be carefully tailored.[68] Pursuing these objectives by engaging in the functionalization of CPs by incorporating specific properties and the utilization of novel FCP materials for SC layers is a highly active area within the realm of potentiometry.

CPs form a network of interconnected molecular wires, where every monomeric unit can be modified with diverse prosthetic groups. By adjusting the properties of these groups, specific interactions with external physical or chemical processes can be caused within these materials. This allows for the creation of molecular devices such as sensors, transducers, *etc.*[118] In general, inorganic compounds possess notable chemical and thermal stability, enabling their utilization in diverse operating conditions. Moreover, they can be acquired through cost-effective processes and deposited as thin or thick films using various techniques. On the other hand, organic compounds offer remarkable synthetic adaptability and reactivity, allowing for manipulation of the molecular structure of sensing materials. This capability enhances the selectivity towards a specific analyte of interest.[119] The idea of combining a CP with an inorganic host has been put forward to create new hybrid materials that possess a combination of the distinctive properties found in semiconducting organic polymers and the mechanical strength and chemical properties typically associated with inorganic materials.[47] As well, the amalgamation of CPs with other organic materials exhibiting specific desired attributes has occurred. To illustrate, metals, metal oxides,[47] and carbon-based materials like carbon nanotubes, graphene, and fullerenes have been combined with CPs to create novel SCs. These functionalized composite materials enable sensors to achieve excellent sensing performance by leveraging the synergistic effects of their components.[47] The synergistic effect of functionalized materials arising from non-electrostatic interactions leads to enhanced electron transfer between substrate and CP, resulting in improved electrocatalytic activity surpassing that of intrinsic CPs. This holds significance in electrochemical sensors, enabling enhanced signal amplification.[51] Further, enhanced redox capacitance in FCPs can be achieved by combining them with materials like graphene. The synergistic effect fosters a more robust electrically conductive network between different materials in contact with. Additionally, the resulting composites exhibit excellent electrochemical stability, a vital attribute for chemical sensing applications.[51]

The hydrophobic nature of conventional CPs (such as PEDOT and PPy) is inadequate to completely eliminate the presence of water layer at buried interfaces,[81] which is one of the main factors contributing to potential instability.[51] However, enhancing the inherent hydrophobicity of CPs can be achieved efficiently by adjusting the counter ion doping and compositing with hydrophobic materials such as carbon nanotubes (CNTs).[81] These composites can be engineered as a compact surface structure, effectively serving as barriers against water and gases (CO_2 and O_2). As a result, they mitigate water infiltration into the underlying electrode substrate.[51] Furthermore, this serves as an example of the application of nanotechnology in augmenting CP capabilities *via* functionalization. By incorporating nanoscale structures, such as nanoparticles or nanotubes, into the CP matrix, the resulting composite materials exhibit improved conductivity, stability, and tailored properties.[120] These nanoscale components provide high surface area, enabling efficient charge transfer and interactions with analytes, thereby enhancing the performance of CP-based SCs. Boosting the specific surface area is a highly effective method for improving capacitance performance.[121] The control of specific surface area can be achieved through the creation of micro-/nanostructures[108] or the integration of nanomaterials.[122] In recent times, the integration of nanotechnology with ISEs has prompted the exploration of numerous strategies for developing fully calibration-free ISEs. One such approach involves utilizing CP nanoparticles, which offer a promising solution for

creating sensors with remarkable potential stability and consistent calibration curves.[123]

These enhancements are anticipated to bolster the electrical and analytical parameters. Comparatively, FCP-based SCs exhibit exceptional qualities such as high potential stability, reproducibility,[51] redox capacitance, a Nernstian slope in the calibration line, a wide dynamic response range, and swift response times.[26] The upcoming sections detail how different CPs are used as SCs with enhanced properties achieved through functionalization.

5.3.1 PPy-based ion-to-electron transducers. PPy exhibits excellent electrical conductivity, structural stability, environmental resistance, biocompatibility, and biodegradability.[124] PPy is extensively utilized as an SC material; for example, Quan *et al.* developed an SC-ISE for the determination of K^+ ions that exhibited a linear response. Electropolymerized PPy film was used as the internal SC layer between the reference element and the ion-sensing membrane.[36] As well, Schwarz *et al.* reported a SC-ISE for the determination of NO_3^- and NH_4^+ in environmental samples, developed with PPy as the ion-to-electron transducer.[125]

PPy composites as SC materials can be tailored to improve properties to be used in SC-ISEs. In this context, Yu *et al.* developed ISE for K^+ using PPy/zeolite (PPy/H-ZSM-5) composites as SC and presented the combination of CPs with zeolites like inorganic materials is promising in creating novel SCs for ISEs, as it enables the integration of both organic and inorganic materials. Electro-synthesized PPy polymer composites have been combined with aluminosilicate inorganic materials and microporous zeolite. During the reaction, the anionic groups present on the zeolite framework served as the counter ions for PPy. The developed PPy/zeolite composite-based K^+-ISE was compared with PPy(Cl^-) based K^+-ISE and the study revealed that the redox capacitance of the PPy/zeolite composites can be more effectively harnessed compared to that of PPy(Cl^-) when coated with a plasticized PVC membrane. Since the Si : Al molar ratio in zeolites can affect the composite's properties, three zeolite composites were examined, with SiO_2/Al_2O_3 ratios of 23, 80, and 280 (Fig. 5a) and higher concentrations of anionic groups in zeolites were found to enhance the deposition of PPy onto their framework, leading to increased conductivity in the composite (Fig. 5b). The PPy/zeolite composite based K^+-ISE showed similar potential stability as the PPy(Cl^-) based K^+-ISE. However, after undergoing a prolonged conditioning period PPy/zeolite composite based K^+-ISEs showed enhanced detection limits.[26] In 2023, Tamara *et al.* reported an ASS-electrode for the determination of tannic acid utilizing PPy–carbon black composite as an ion-to-electron transducer which encompasses the redox-active nature of PPy and properties of carbon black such as inert nature, high specific surface area, hydrophobicity and high double-layer capacitance. The addition of the PPy–carbon black composite layer noticeably enhanced the sensor's stability due to its high capacitance. There was no presence of a water layer beneath the membrane, and the sensor remained stable even in the presence of O_2 and light.[126]

A significant issue concerning CPs is that the high charge density in the oxidized state inducing the formation of the aqueous layer. He *et al.* introduced a resolution to this issue by incorporating a remarkably hydrophobic perfluorinated anion, specifically perfluorooctanesulfonate ($PFOS^-$), as a doping ion. This choice renders the oxidized form of the CP to be hydrophobic. They have successfully developed a K^+-SC-ISE utilizing PPy films doped with $PFOS^-$ (PPy-PFOS) as the SC. The SC was subjected to a pre-polarization process before applying.[91] CPs have varying energy levels due to polymer segments of different conjugation lengths, making it difficult to achieve consistent E° reproducibility in SC-ISEs. Thus, pre-polarizing the SC at a specific potential within the conducting range is necessary to enhance the reproducibility of CP-based SC-ISEs.[127] FTIR-ATR spectra of PPy-PFOS revealed a notably sluggish water absorption rate for the SC (Fig. 5c). The K^+-SC-ISE demonstrated remarkable E° reproducibility, with a minimal deviation of only $\pm$0.7 mV. This reproducibility can be attributed to the combination of the pre-polarization of PPy-PFOS SC and its exceptional water barrier properties, owing to its high hydrophobicity.[91]

Leveraging the intriguing physicochemical properties of carbon nanotubes (CNT), such as their high electrical conductivity, mechanical strength, thermal conductivity, and surface area, with PPy, Abbaspour *et al.* have designed composite material as an ion-to-electron transducer. The Ag^+-SC-ISE with PPy-multiwalled carbon nanotubes (PPy-MWCNTs) composite SC gave better performance with a Nernstian slope of 59.4 $\pm$ 0.5 mV per decade over a wide linear concentration range of 1.0×10^{-7} to 1.0×10^{-1} mol L^{-1} (Fig. 5d). Incorporating MWCNTs into a polymer matrix enhances the electrode's linear range and sensitivity. Additionally, the composite film displayed a smoother and more uniform surface compared to the MWCNTs alone (Fig. 5e).[120]

5.3.2 PANI-based ion-to-electron transducers. Due to its straightforward electrochemical synthesis and impressive electronic/ionic conductivities, PANI has been extensively utilized as a CP in SC-ISEs.[81] PANI has three different forms: leucoemeraldine, pernigraniline, and emeraldine with different oxidation states and protonation levels.[53,87] Out of these three forms, only the emeraldine form exhibits conductivity.[87] Even though, PANI is sensitive to the pH changes,[103] PANI demonstrates excellent stability both in the presence of air and moisture.[128] PANI-based materials have received significant attention due to the unique characteristics of PANI and the synergistic effects observed in composites.[129–131] Pietrzak *et al.* presented the development of NO_3^--SC-ISE utilizing PANI nanofibers doped with chloride (PANI NFs-Cl) and nitrate (PANI NFs-NO_3) ions as SCs. The utilization of PANI nanofibers consisting of relatively cohesive structures (Fig. 6a) was discovered to have a beneficial impact on the performance of potentiometric sensors, notably enhancing the stability and reversibility of the electrode potential (Fig. 6b). Both types of sensors utilizing Cl-doped PANI nanofibers and NO_3^--doped PANI nanofibers as an intermediate layer were capable of operate in solutions with a broad pH range (4.0–12.5) and under variable lighting conditions and in the presence of dissolved gases such as O_2. As

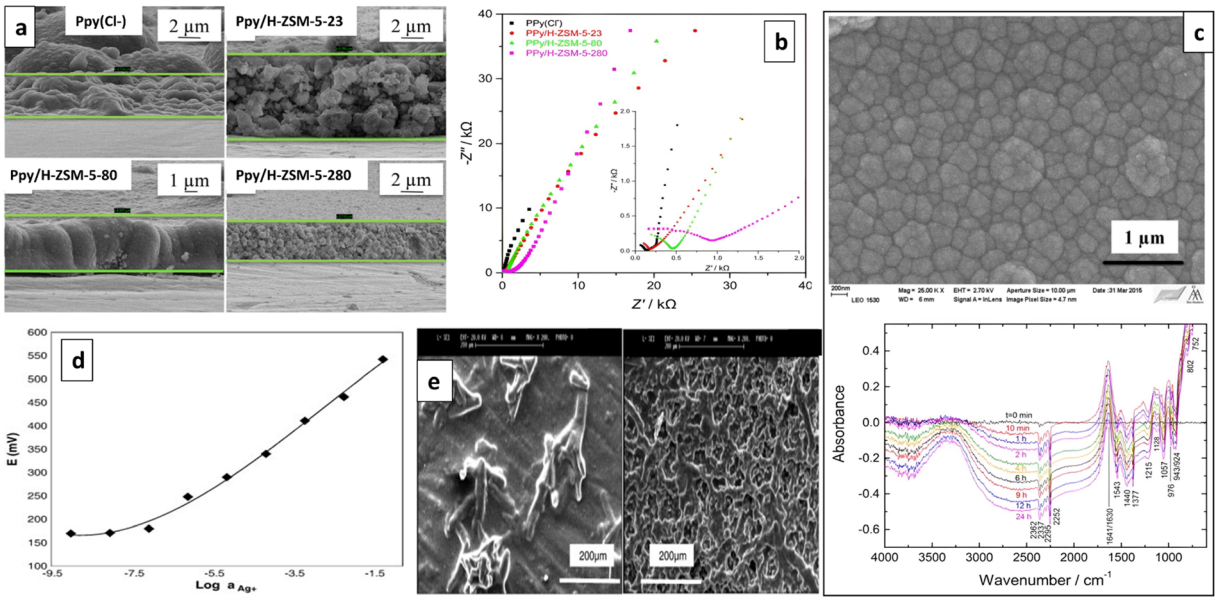

Fig. 5 (a) SEM micrographs and (b) impedance spectra of PPy/Cl^- and PPy/zeolites SCs. Reproduced with permission.[26] Copyright 2017, Elsevier. (c) SEM micrograph of pre-polarized PPy-PFOS film (upper) and its FTIR-ATR spectra during water uptake (lower). Reproduced with permission.[91] Copyright 2017, American Chemical Society. (d) Potential response of PPy-MWCNTs SC-ISE and (e) SEM micrographs of MWCNTs (left) and PPy-MWCNTs composite (right). Reproduced with permission.[120] Copyright 2014, Elsevier.

well, the electrodes demonstrated favourable long-term stability.[53]

The characteristics of PANI can be adjusted by incorporating additional functional groups into the monomer, resulting in PANI derivatives that may be more suitable for application in ISEs.[128] Liu *et al.* introduced a new approach to enhance the potential stability and improve the detection limit of SC-ISEs by utilizing electrospun PANI (s-PANI)/polymethyl methacrylate (PMMA) microfibers as an ion-to-electron transducer for glassy carbon (GC)/s-PANI/Pb^{2+}-ISE. The GC/s-PANI/Pb^{2+}-ISE exhibited increased capacitance and reduced impedance, indicating faster ion-to-electron transportation compared to the drop-coated GC/d-PANI/Pb^{2+}-ISE which contains microparticles. This can be attributed to the s-PANI/PMMA possessing homogenous and larger specific surface area as depicted in the SEM micrographs (Fig. 7a). The s-PANI microfibers effectively

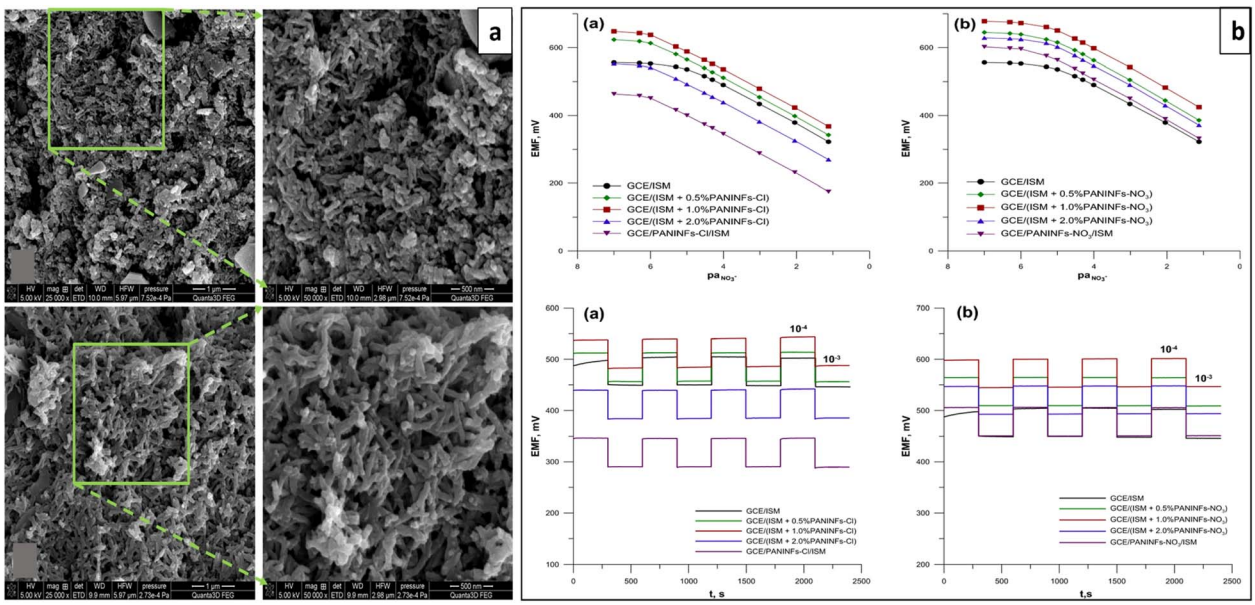

Fig. 6 (a) SEM micrographs of PANI NFs-Cl (upper) and PANI NFs-NO_3 (lower) and (b) ISE performances. Reproduced with permission.[53] Copyright 2021, Springer.

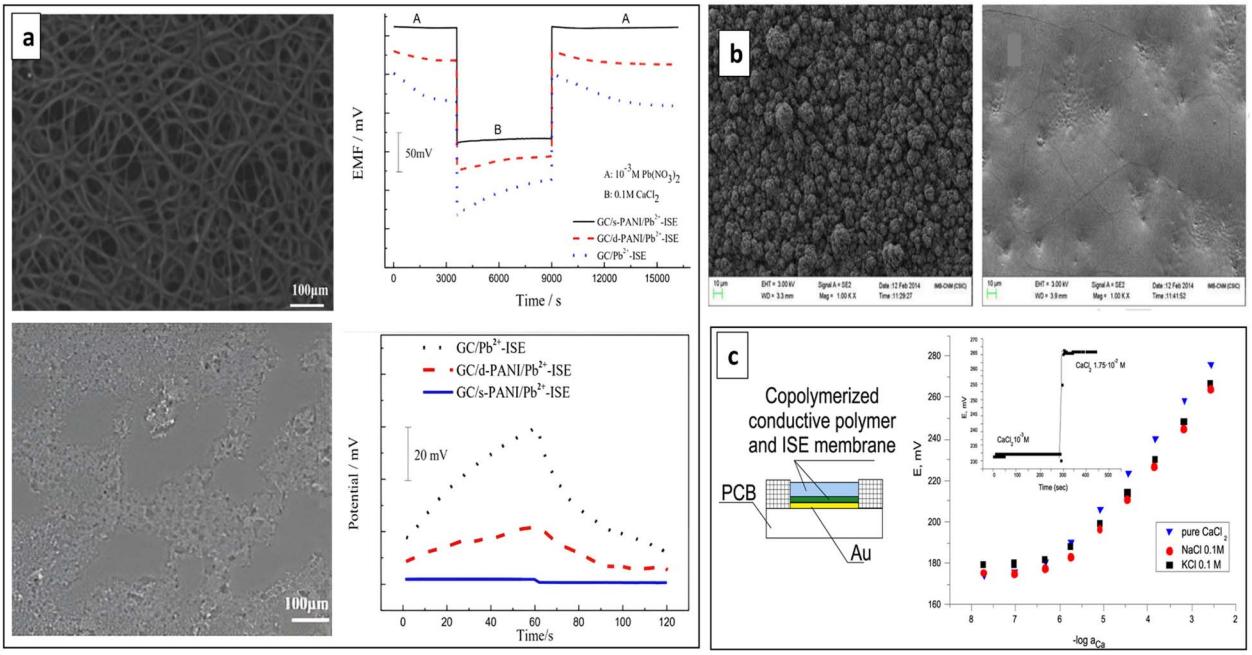

Fig. 7 (a) SEM micrograph of s-PANI (upper) and d-PANI (lower) coatings and comparison study of performances of bare GC electrode and ISEs with d-PANI SC and s-PANI SC (potential stability and potentiometric water layer test). Reproduced with permission.[132] Copyright 2017, Elsevier. (b) SEM image of PANI-DBS (left) and P-NPEDMA-DBS (right) surfaces. (c) Schematic illustration and performances of the ISE with P-NPEDMA-DBS SC. Reproduced with permission.[133] Copyright 2016, Elsevier.

reduce the transduction resistance between the substrate and ISM. Moreover, the GC/s-PANI/Pb^{2+}-ISE demonstrated the elimination of the interfacial water film in the water layer test (Fig. 7a). This is attributed to the stronger and more robust adhesion between the ISM and s-PANI contact. The GC/s-PANI/Pb^{2+}-ISE exhibited high potential stability, ability to detect concentrations as low as 6.3×10^{-10} M within a range of 10^{-9}–10^{-3} M $Pb(NO_3)_2$, and a response time of less than 10 seconds.[132] Abramova *et al.* developed a SC-ISE featuring a SC that is stable and long-lasting, effectively inhibiting the formation of a water layer at the interface between the ISM and the SC. They introduced a novel approach that involves the simultaneous copolymerization of the CP layer and the polyurethane acrylate matrix of the ISM. This copolymerization, which occurs in a single photopolymerization step, chemically bonds the ISM to the CP while incorporating the typical additives; ionophore and ion exchanger. In their study, they investigated a bifunctional monomer called *n*-phenyl-ethylenediamine-methacrylamide (NPEDMA), which consists of an aniline group linked to a methacrylamide group and employed as an SC layer in a SC-ISE for Ca^{2+}. Upon polymerization, the surface of NPEDMA displayed a dense concentration of methacrylamide groups, which served as reactive sites for improved bonding and enhanced adhesion to the acrylate membrane. P-NPEDMA-4-dodecylbenzenesulfonic acid (P-NPEDMA-DBS) film exhibits a notably smoother surface (Fig. 7b), which can be advantageous as smooth films have demonstrated greater stability in potentiometric sensors compared to rough counterparts. The developed ISE exhibited a Nernstian response (Fig. 7c), enhanced potential stability, and absence of pH sensitivity within pH range of 4–9. Further, copolymerization of the two layers creates strong adhesion, preventing the formation of water layers at the interface between the ISE membrane and the SC.[133]

Recently in 2019, Jiang *et al.* reported a Pb^{2+}-SC-ISE developed using hydrophobic PANI-polystyrene (PANI-PS) microfiber films as the ion-to-electron transducer through electrospinning (e-PANI-PS). It exhibited 104° of water contact angle indicating high hydrophobicity that can be ascribed to its rich texture and roughness (Fig. 8a). Further, it demonstrated better analytical performances including a wide linear detection range of 10^{-8} to 10^{-3} mol L^{-1}, a low detection limit of $\sim 5 \times 10^{-9}$ mol L^{-1}, a Nernstian slope of 29.1 mV per decade and a fast response time of <10 s. It was revealed that compared to PANI microfibers or drop-cast PANI-PS films as the ion-to-electron transducers, e-PANI-PS exhibited lower detection limit and better stability that can be attributed to its high hydrophobicity, higher capacitance, and lower impedance that enable the fast ion-to-electron transport. However, a small potential disturbance was noticed for O_2 and CO_2, and light exposure had no significant impact.[134]

To improve the potential stability *via* enhancing effective ion-to-electron transduction process, Zeng *et al.* developed Pb^{2+}-SC-ISE using PANI doped with titanium dioxide (PANI-TiO_2) as the SC that possesses a large specific capacitance. The semiconducting nature of TiO_2 and its ability to versatile fabrication into diverse complex morphologies can enhance capacitance. The PANI-TiO_2 films displayed irregular textured surfaces due to blended TiO_2 powders with PANI, resulting in a rougher surface (Fig. 8b). This roughness increased adsorption sites for sodiumtetrakis [3,5-bis(trifluoromethyl)phenyl]borate

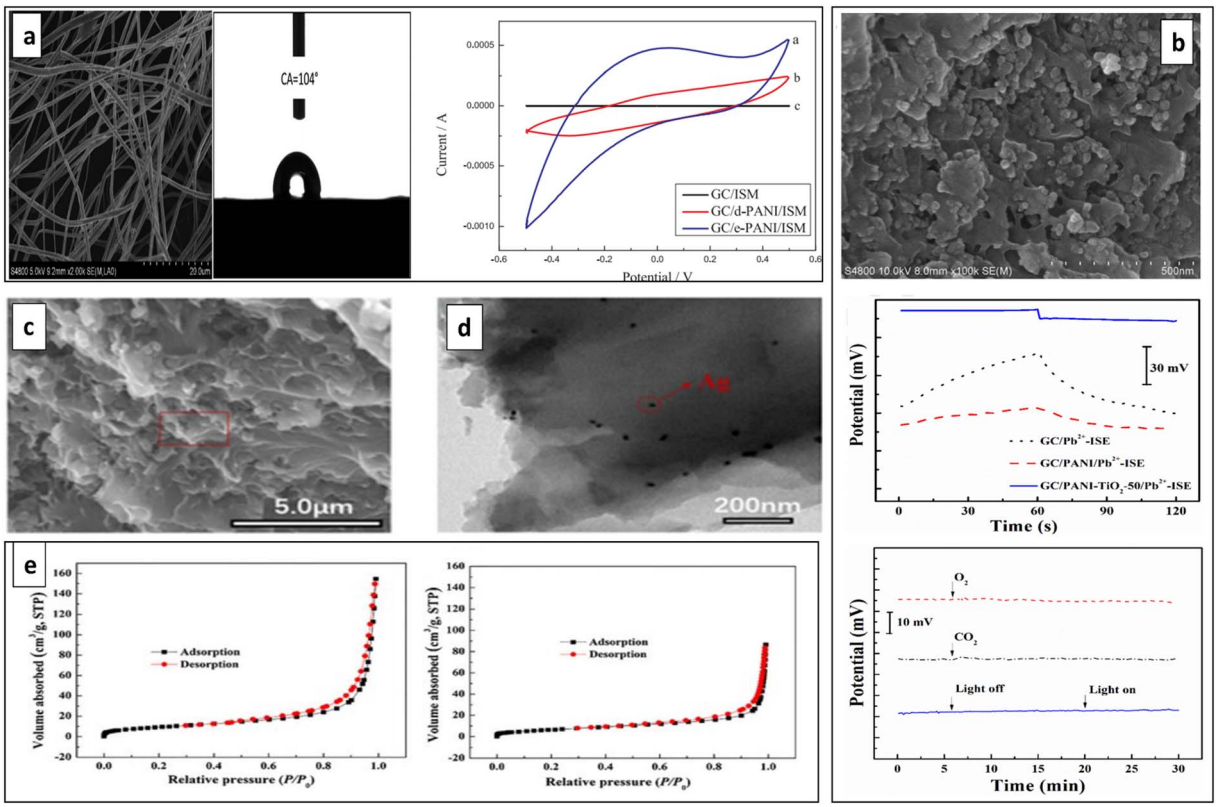

Fig. 8 (a) SEM micrographs and water contact angle of e-PANI films. Cyclic voltammograms of three different electrodes (bare GC, with d-PANI SC and with e-PANI SC). Reproduced with permission.[134] Copyright 2019, Elsevier. (b) SEM micrograph of PANI-TiO_2 composite material, potential stability, light and gas sensitivity of electrodes. Reproduced with permission.[135] Copyright 2020, Elsevier. (c) SEM and (d) TEM images of AgNPs-PANI. (e) N_2 adsorption–desorption isotherms for AgNPs-PANI (left) and PANI (right). Reproduced with permission.[136] Copyright 2021, Springer.

(NaTFPB) of ISM, boosting electrode capacitance. This enhanced capacitance helps stabilize electrode potential. Consequently, compared to the PANI which has smooth surfaces, the textured PANI-TiO_2 more effectively converted ionic signals from Pb^{2+} into electrical signals. The developed ISE showed a stable and rapid potential response to Pb^{2+} ions, with a linear range from 10^{-3} to 10^{-9} M, a detection limit of approximately $10^{-9.1}$ M, and a quick response time of only 10–15 s. Additionally, it exhibited a small potential drift of 122.6 μV s^{-1} and remained stable over time.[135] The performance improvement can be attributed to the semiconducting nature of TiO_2 and its ability to be fabricated in various complex morphologies.[137–140]

Metal nanomaterials have garnered significant interest in recent years for their intriguing optical and electron transfer characteristics.[141] This has resulted in their extensive use across chemical and biological sensing.[136] Among these, silver nanoparticles are of particular interest for establishing unique charge transport pathways.[142] Composite materials of CPs and metal nanoparticles hold potential as ion-electron transport layers in ISEs due to their exceptional conductivity and substantial specific surface areas.[143] Recently in 2021, Zeng *et al.* developed a Pb^{2+}-SC-ISE utilizing composite prepared with Ag nanoparticles and PANI (AgNPs-PANI).[136] AgNPs-PANI composite serves as an effective strategy for enhancing electron transfer reactions between SC and conductive substrates.[144] Due to the synergistic effects of Ag nanoparticles and PANI, the AgNPs-PANI SC exhibited high capacitance and excellent electron transport performance. AgNPs-PANI consisted with a rough surface morphology (Fig. 8c) and uniformly dispersed AgNPs (Fig. 8d). The high capacitance of AgNPs-PANI resulted from its larger specific surface area compared to the PANI film (Fig. 8e). The developed sensor demonstrated excellent performance with a low detection limit of 6.31×10^{-10} M, a slope of 29.1 ± 0.3 mV per decade, and a fast response time of less than 5 seconds. It showed high short-term and long-term potential stabilities. As well, Nernstian response for Pb^{2+} ions across a wide concentration range (10^{-3} to 10^{-9} M).[136]

Recently, using synergistic effects of graphene and PANI, Boeva *et al.* developed a SC and applied in Ca^{2+}-SC-ISE.[51] Here, the formation of a more extensive electrically conductive network between graphene and CP resulted in greater redox capacitance of PANI-graphene composite SC than PANI SCs.[145] Graphene-like carbon materials enhance the reproducibility/stability of the $E°$ which can be attributed to their relatively ample surface area that reduces their susceptibility to small variations in double-layer capacitance. The PANI-graphene composite-based SC-ISEs are characterized by high

electrocatalytic activity compared to intrinsic PANI-based SC-ISEs. Graphene increased the transducer's hydrophobicity with reported higher water contact angle ultimately preventing water layer formation. Additionally, it exhibited excellent potential reproducibility of only ±4 mV ($n = 3$), a low detection limit of 5×10^{-8} M, and good electrochemical stability.[51]

Pietrzak *et al.* reported the use of a nanocomposite consisting of chloride-doped PANI nanofibers and multiwalled carbon nanotubes (PANI NFs-Cl:MWCNTs) as a SC for constructing a Cl^--SC-ISE. The ISE showed a theoretical slope of −61.3 mV per decade in its electrode characteristic curve, a wide linear range from 5×10^{-6} to 1×10^{-1} mol L^{-1}, and excellent potential stability even under varying measurement conditions such as in the presence of light and O_2. The achieved favourable sensing properties can be ascribed to the combination of PANI nanofibers and MWCNTs resulting in a nanocomposite that consisted of PANI nanofibers entwined by CNTs (Fig. 9a). The electrode is characterized with low resistance and high capacitance.[76]

There is a considerable demand to miniaturize ion sensors for wearable, health, and sports applications. This is primarily accomplished through the printing of SC-ISEs on paper and other flexible, stretchable substrates. FCPs can facilitate the creation of affordable and straightforward wearable technologies which are increasingly widespread. Rutkowska *et al.* developed a cost-effective, flexible, and miniaturized K^+-SC-ISE on laminated graphene paper substrate that can be used in wearable applications (Fig. 9b). For optimal performance, the SC should ideally be resistant to pH changes, thus minimizing potential drifts due to proton diffusion from the ISM to the SC. Such diffusion can induce pH-related potential alterations, primarily at the interface between the SC and the ISM. Here, a miniature ISE containing PANI doped with dinonylnaphthalene sulfonic acid (DNNSA) as the SC has been reported.[146] Doping PANI with bulky dopants like DNNSA caused to strongly supress the inherent pH sensitivity of PANI.[147] The sensor demonstrated a Nernstian slope of 56.9 ± 0.1 mV pK^{-1}, with a high E^o reproducibility of ±4.4 mV even after more than 24 hours. It exhibited excellent selectivity against Na^+, Li^+, H^+, Mg^{2+}, and Ca^{2+}, and it was not sensitive to water, light, or oxygen gas. However, there was a slight response to CO_2 due to pH sensitivity of PANI.[146]

To improve the potential stability of NH_4^+-ISEs, Bao *et al.* recently developed superhydrophobic SC by doping PANI with perfluorooctanoic acid (PFOA). It demonstrated outstanding potential stability against external interferences and during wastewater monitoring, featuring a slope of 58.07 mV per decade, which closely aligns with the ideal Nernstian slope and exhibits a minimal potential drift of only 13.6 ± 3.2 μV h^{-1}.[148] A common practice involves combining CPs with single metal oxide nanoparticles to serve as effective ion-to-electron transducers. Notably, in 2023, Abdallah *et al.* developed a bimetallic/PANI nanocomposite as a transducer by utilizing TiO_2 and CuO nanoparticles, encapsulated within a PANI shell, for the determination of Vildagliptin (Fig. 10a). This innovative approach results in a nanocomposite with a significant surface area, increased chemical stability, and robust mechanical strength. The metal oxide nanoparticles function as fillers, effectively modifying the properties of PANI, facilitating the creation of an ordered structure within PANI, and augmenting its electrical and sensing capabilities compared to pristine PANI (Fig. 10b and c). The bimetallic/PANI nanocomposite exhibited superior

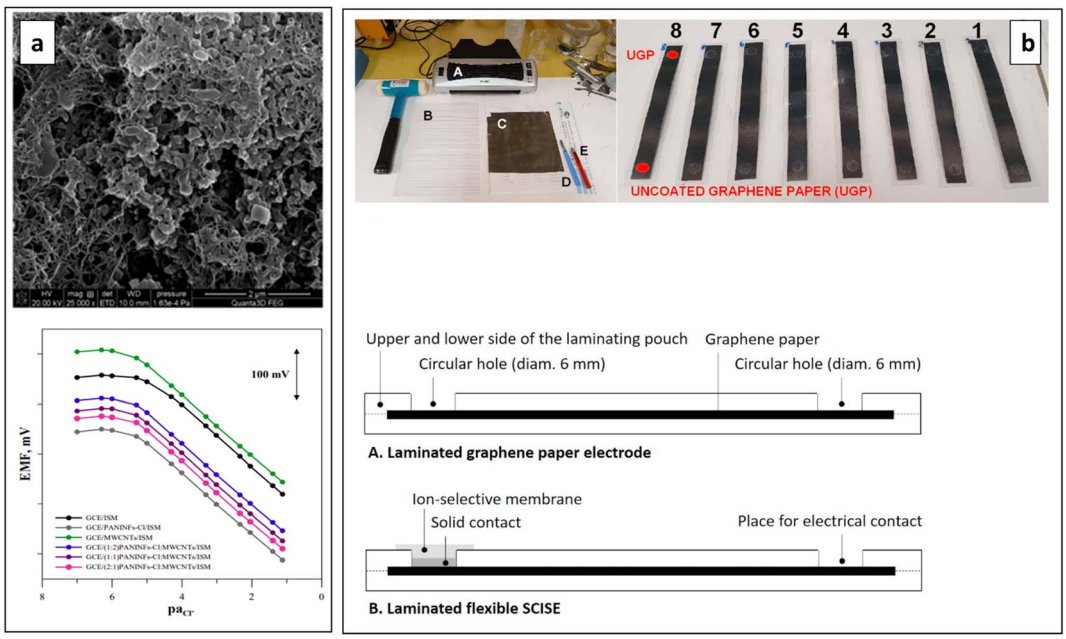

Fig. 9 (a) SEM image of PANI NFs-Cl: MWCNTs composite (upper) and potentiometric responses of the SC-ISEs (lower). Reproduced with permission.[76] Copyright 2022, MDPI, Basel, Switzerland. (b) Required equipment for the fabrication process, laminated graphene paper electrodes (upper) and schematic side view of the flexible SC-ISEs (lower). Reproduced with permission.[146] Copyright 2021, Elsevier.

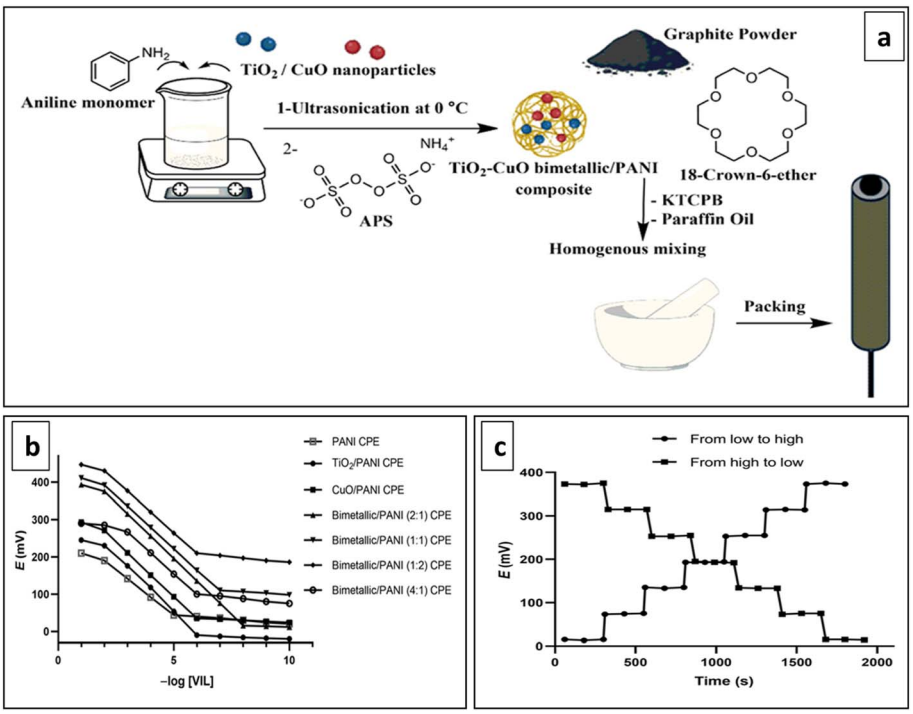

Fig. 10 (a) Diagram outlining the fabrication process of the electrode with TiO_2–CuO bimetallic/PANI nanocomposite transducer, (b) potentiometric responses and (c) dynamic response time of the electrode. Reproduced with permission.[149] Copyright 2023, MDPI, Basel, Switzerland.

physical, chemical, and catalytic activity, integrating properties of both metal oxides with PANI, featuring a wide linear range (10^{-2}–10^{-8} M), excellent sensitivity, and a notably enhanced lower detection limit (4.5×10^{-9} M) in contrast to composites utilizing single metal oxide nanomaterials.[149]

5.3.3 PEDOT-based ion-to-electron transducers. PEDOT is recognized as a highly promising CP due to its high conductivity, moderate bandgap, good environmental stability, biocompatibility, and high optical transparency.[150] PEDOT holds significant potential as an ion-to-electron transducer for SC-ISEs among other members in the CP family. This is due to PEDOT's advantageous characteristics of lower electroactivity and reduced occurrence of electrochemical side reactions compared to highly p-doped CPs. Furthermore, the high conductivity of PEDOT can potentially contribute to the prevention of water and salt accumulation between the conductive substrate and the ISM.[65] PEDOT is a redox CP.[81] PEDOT and PEDOT doped with poly (styrenesulfonate) (PSS) have been identified as exceptionally stable CPs, primarily attributed to their minimal susceptibility to O_2 and CO_2 (pH) changes.[55,73,151]

To ensure potential reproducibility Papp *et al.* developed a K^+-SC-ISE using perfluorinated alkanoate side-chain functionalized PEDOT (PEDOTF) as a hydrophobic SC. In order to enhance the E° reproducibility and to ensure the thermodynamic reversibility at the interface between the SC and ISM, the lipophilic additive present in ISM which is tetrakis(pentafluorophenyl)borate ($TFAB^-$) anion has been incorporated into the SC. The pre-polarization of the PEDOTF-TFAB transducer before the deposition of the ISM resulted in an exceptionally stable open-circuit potential and outstanding potential reproducibility (Fig. 11a). As well, it consisted of a water contact angle of 133° demonstrating the high hydrophobicity of the oxidation state of PEDOTF-TFAB which remains consistent over time and can be accurately adjusted through pre-polarization. The hydrophobic nature is influenced by the uniform surface morphology with an open surface structure, featuring distinct polymer bundles extending outward from the surface (Fig. 11a).[117]

For single-use/disposable sensors intended for *in vivo* or field applications, concise conditioning is particularly significant. Recently, Guzinski *et al.* studied the effect of the thickness of poly(3,4-ethylenedioxy thiophene):polystyrene sulfonate (PEDOT:PSS) SC on the equilibration times. They found that using the optimum thickness of the PEDOT(PSS) SC layer, it is possible to achieve SC-ISEs eliminating the need for extensive conditioning. This occurs due to the potential drifts associated with the PEDOT(PSS) film and substrate|PEDOT(PSS) interface are counteracted by potential drifts of opposite polarity at the PEDOT(PSS)|ISM interface and within the ISM.[155]

To develop cost-effective and straightforward SC-ISEs with potential commercial applications, Ocana *et al.* conducted a comparative study involving six different commercially available conducting materials. These materials include polypyrrole-*block*-polycaprolactone (PPy-*b*-PCaprol), graphene/poly(3,4-ethylenedioxythiophene): poly(styrenesulfonate) (graphene-PEDOT:PSS) ink, poly(3,4-ethylenedioxythiophene):polyethylenglycol (PEDOT:PEG), high conductivity PEDOT:PSS, and polyethylenimine (PEI) with PEDOT:PSS. The purpose of this study was to evaluate their potential as ion-to-

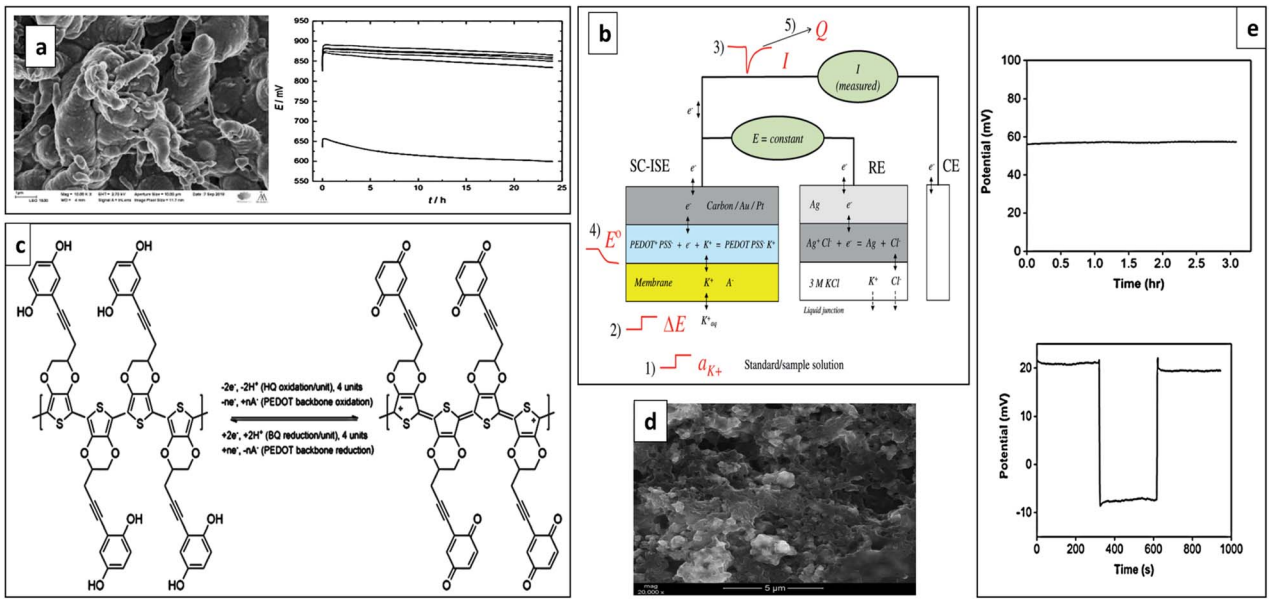

Fig. 11 (a) SEM image of PEDOTF SC and performances of K^+-SC-ISE having PEDOTF SC (initial potential stability and reproducibility). Reproduced with permission.[117] Copyright 2019, American Chemical Society. (b) Schematic representation of the novel ion-to-electron transduction principle using a three-electrode cell (working electrode as ISE using PEDOT: PS, CE is the counter electrode and RE is the reference electrode). Reproduced with permission.[152] Copyright 2015, Wiley-VCH Verlag GmbH & Co. KGaA, Weinheim. (c) Redox processes of PEDOT and HQ/BQ pendant groups. Reproduced with permission.[127] Copyright 2021, Elsevier. (d) SEM image of RuO_2-PEDOT:PSS composite. Reproduced with permission.[153] Copyright 2021, MDPI, Basel, Switzerland. (e) Long-term stability and reversibility of calibration-free ISE for K^+ and Ca^{2+}. Reproduced with permission.[154] Copyright 2022, American Chemical Society.

electron transducers in polyurethane-based pH-SC-ISEs and it was found that out of all, the electrodes based on PEDOT:PEG demonstrated the most favourable outcomes in terms of sensitivity, reproducibility, and longevity with the highest redox capacitance.[38] Recently, in 2022, Neo *et al.* reported the NO_3^--SC-ISE using PEDOT:PEG as a solution-printable SC. It showed improved sensor performances with nearly Nernstian response of −55.8 mV per decade over a broad concentration range of 0.1 M to 1.12 µM.[156]

In the realm of pH sensing, particularly in clinical diagnostics, the inclusion of a water layer in SC-ISEs poses a significant risk of introducing errors. This is due to the fact that the concentration of CO_2 in blood can fluctuate within a range of approximately 20 to 80 mmHg under normal physiological conditions at 37 °C. Guzinski *et al.* have used superhydrophobic counter ion tetrakis(pentafluorophenyl)borate ($TPFPhB^-$) doped functionalized PEDOT with C_{14} alkane chain (PEDOT-C_{14}) as ion-to-electron transducer for developing SC-ISE for pH sensing without interference from CO_2. It exhibited exceptional performance attributes including theoretical response slope, long-term potential stability (0.02 ± 0.03 mV per day), and reproducibility of ±0.002 pH unit. Further, it exhibited enhanced interfacial hydrophobicity, as evidenced by a contact angle measurement. The pH sensors developed with PEDOT-C_{14}(TPFPhB) as the SC, exhibit comparable long-term potential stability due to the incorporation of colloid-imprinted mesoporous carbon. These electrodes are renowned for their exceptional potential stability, surpassing all other SC-ISEs, with a reported drift of approximately 31 µV per day.[157]

The utilization of 3D structure of CP to significantly increase the redox capacitance, ultimately enhancing the reproducibility of SC-ISE was recently reported by Szucs *et al.* This group of researchers has developed an SC-ISE for Ag^+ ions using PEDOT(PSS) films with 750 nm diameter interconnected pores as the SC layer, using 3D nanosphere lithography and electrosynthesis to achieve a high surface area and capacitive interface. This film exhibited a redox capacitance nearly seven times larger than the film created through direct electrosynthesis. Additionally, the 3D PEDOT(PSS) film was modified with a lipophilic redox couple (1,10-dimethylferrocene) to further enhance both the redox capacitance and hydrophobicity. As a result, better electrode-to-electrode reproducibility with low standard deviation for $E°$ was demonstrated.[158]

Potential instability is a frequent problem in classical potentiometric measurements for SC-ISEs. To address this, Hupa *et al.* proposed an alternative ion-to-electron transduction principle for SC-ISEs that involves keeping the potential of the SC-ISE constant. The suggested signal transduction method was demonstrated successfully using a K^+-ISE model sensor. The sensor utilized PEDOT doped with PSS as the SC. In contrast to the traditional phenomena applied in SC-ISEs, where ion activity is determined by the zero-current potential relative to the reference electrode, the suggested signal transduction principle is similar to "constant-potential coulometry". It utilizes the redox capacitance of the internal SC to convert variations in ion concentration (activity) into an electrical current (Fig. 11b).[152]

In 2020, Ivanko *et al.*, developed a light, O_2, and CO_2 insensitive K^+-SC-ISE using PEDOT with covalently attached hydroquinone (HQ) pendant groups to the polymer backbone (PEDOT-HQ) as the SC (Fig. 11c). In PEDOT-HQ, the covalently attached HQ groups prevent leaching that leads to potential drift and potential irreproducibility and enable approximately 25–30 times higher charge storage and high redox capacitance of 490 mF cm^{-2} compared to unsubstituted PEDOT. However, the presence of water at the inner electrode interfaces was observed, likely due to the hydrophilic nature of the HQ pendant groups.[127]

Doping PEDOT composites with different nanomaterials has enhanced their properties.[122,143,159] In this context, Lenar *et al.* developed a K^+-SC-ISE using a nanocomposite material of PEDOT:PSS with ruthenium dioxide (PEDOT:PSS-RuO_2), effectively combining the properties of both compounds to achieve efficient conductivity for transduction processes and high electrical capacity. The nanocomposite layer consisted of high surface area (Fig. 11d) leading to an impressively high electrical capacitance, reaching approximately 17.5 mF, resulting in excellent performance. The ISE demonstrated rapid and stable potentiometric responses across a wide range of potassium ion concentrations (10^{-6} M to 10^{-1} M), with a minimal potential change of only 0.077 mV per hour.[153]

Recently, there has been a significant surge of interest in wearable technology for health monitoring.[160–163] SC-ISE designed for portable and wearable analytical applications, commonly employs CPs to facilitate ion-to-electron transduction. Liu *et al.* introduced an integrated wearable sensor, founded on SC-ISE technology, employing PEDOT:PSS as the ion-to-electron transducer with remarkably consistent E° values, for real-time detection of Na^+ and K^+ ions in human sweat. The sensor achieved E° repeatability by applying a positive potential with a short pre-treatment, resulting in increased oxidation of the CP's redox state. The developed SC-ISEs demonstrated excellent multi-use performance without the need to switch electrodes or perform rinsing treatments.[111]

Bahro *et al.* developed a calibration-free ISE for K^+ and Ca^{2+} determination in water samples by designing a SC using a combination of 3,4-ethylenedioxythiophene (EDOT) and 4-(2,3-dihydrothieno[3,4-*b*][1,4]dioxin-2-yl-methoxy)-1-butanesulfonic acid, sodium salt (EDOT-S). The PEDOT:PEDOT-S SC charging cycles allowed to set a constant background potential at a desired fixed intercept value for different ionophores. The ISE showed good reversibility, long-term stability (Fig. 11e), Nernstian responses of 57.2 ± 0.2 mV per decade for K^+ and 28.5 ± 0.3 mV per decade for Ca^{2+}, and low detection limits for both ions.[154]

To ensure the E° reproducibility, Kozma *et al.* designed K^+-SC-ISEs featuring a highly hydrophobic SC. This was achieved through the copolymerization of 3,4-ethylenedioxythiophene with a perfluorinated alkyl side chain (EDOTF) and 3,4-ethylenedioxythiophene modified with (2,2,6,6-tetramethylpiperidin-1-yl)oxyl (EDOT-TEMPO) (Fig. 12a). The exceptional hydrophobicity (>130°) reported (Fig. 12b) was attributed to the perfluorinated alkyl side chain, while the electron-to-ion transduction was linked to the CP (EDOT) backbone and the confinement of well-defined redox couple (TEMPO). The K^+-SC-ISEs based on P(EDOTF-EDOT-TEMPO) were found to be unaffected by light, CO_2, and O_2. The minimal potential drift, as low as 0.15 mV h^{-1}, was observed, indicating a high level of potential stability (Fig. 12c).[34]

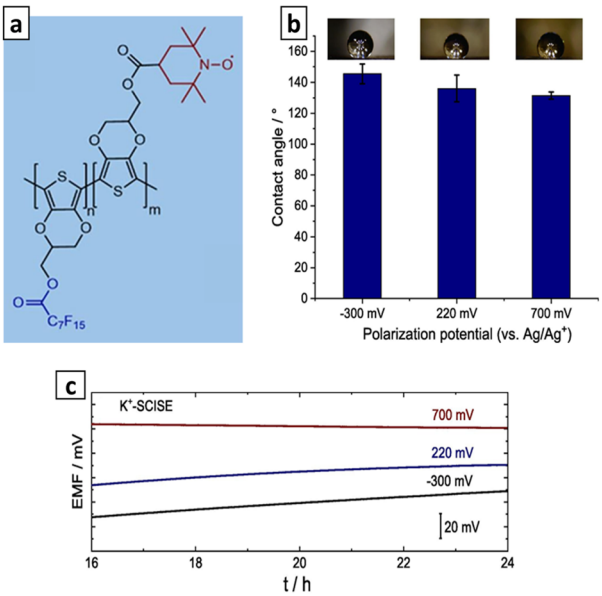

Fig. 12 (a) Molecular structure of P(EDOTF-EDOT-TEMPO), (b) water contact angles and (c) potential stability of conditioned SC-ISEs that SCs were pre-polarized at different potentials. Reproduced with permission.[34] Copyright 2023, Elsevier.

5.3.4 POT-based ion-to-electron transducers. POT is a type of CP that possesses outstanding transducer properties.[164] It is highly hydrophobic and can be easily deposited on the surface of an electrode using methods such as drop casting or electrodeposition. Its involvement in side reactions is minimal.[72] POT plays a role in facilitating small ion exchange/ion-fluxes between the ISM and SC layer, leading to reduced detection limits.[164] Nonetheless, POT has some drawbacks, such as having much lower redox capacity and conductivity.[72] POT is functionalized to surpass these limitations and enhance features. Bao *et al.* developed a K^+-SC-ISE employing POT–carbon black nanocomposite as the transducer. Here, POT is used as the dispersant of carbon black. The superhydrophobicity of carbon black prevents the formation of a water layer ultimately eliminating the instability and drift in the potential of the electrode. Here, integrated the carbon materials' high specific surface area and the high hydrophobicity of POT and carbon black. The nanocomposites possessed high surface roughness (Fig. 13a) and exhibited distinctive features, such as low resistance of electron transfer between the SC|ISM interface, high conductivity, capacitance, and stability. Additionally, the electrode exhibited a low detection limit of $10^{-6.2}$ M, high hydrophobicity with a water contact angle of 139.7° (Fig. 13a), and remains unaffected by light, O_2, and CO_2.[72]

Metal oxides were found to enhance the electrical and analytical characteristics of sensors.[167] Utilizing metal oxides (*e.g.*, ruthenium dioxide, iridium dioxide) as SCs increases the

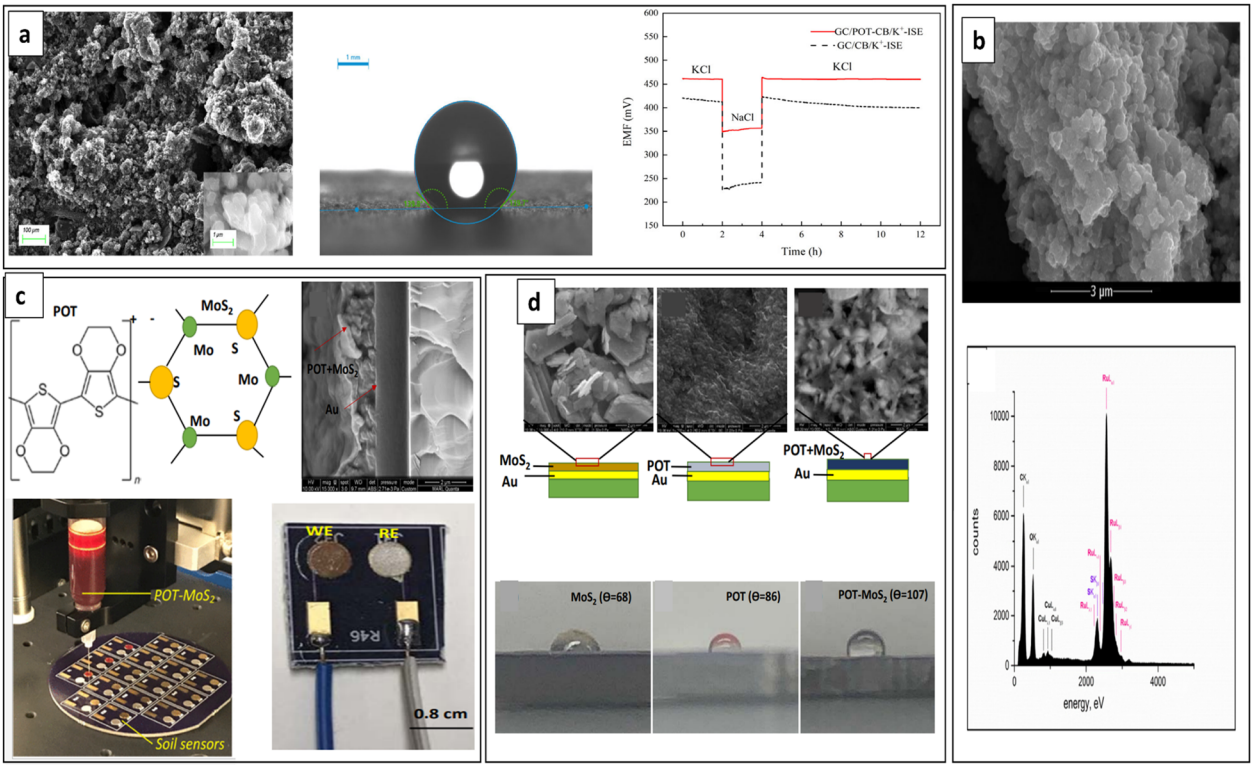

Fig. 13 (a) SEM image and water contact angle of POT–carbon black SC layer and potentiometric water layer test. Reproduced with permission.[72] Copyright 2023, MDPI, Basel, Switzerland. (b) SEM image (upper) and EDAX spectrum (lower) of POT–RuO_2 composite. Reproduced with permission.[165] Copyright 2019, Elsevier. (c) POT–MoS_2 composite transducer-based SC-ISE fabricated with an automatic fluid dispenser for the analysis of NO_3^- ions in the soil. (d) SEM images (upper) and water contact angles (lower) of MoS_2, POT and POT–MoS_2 SC layers. Reproduced with permission.[166] Copyright 2019, American Chemical Society.

electrode electrical capacity and subsequently enhances the potentiometric response stability.[86] Recently in 2019, Lenar *et al.* reported a K^+-SC-ISE using nanocomposite composed of ruthenium dioxide (RuO_2) and POT as the SC. The microstructure analyses proved a coherent composite material (Fig. 13b) and POT–RuO_2 nanocomposite SC exhibited high water contact angle of 149° indicating superhydrophobic behaviour compared to POT alone that has a water contact angle of ~91°. The RuO_2–POT composite material achieved a high electrical capacitance of 1.17 mF, enabling a stable potentiometric response.[165]

Jarvis *et al.* conducted a research study aiming to enhance the potential stability and potential reproducibility of sensor-to-sensor that used POT as the SC layer, by introducing a 7,7,8,8-tetracyanoquinodimethane (TCNQ) salt (such as K^+TCNQ^-) into a POT film. This salt acted as the primary ion for determining the reproducible interfacial potential between POT and ISM, resulting in optimized performance. Through the polarization of the K^+ ISEs, the infused TCNQ/$TCNQ^{\bullet-}$ redox couple ratio in the POT film was adjusted to approximately 1 : 1. This TCNQ/$TCNQ^{\bullet-}$ couple plays a role in stabilizing the potential of the POT film and the interfacial potential between the substrate and POT. In conclusion, this adjustment contributes to the overall improvement in potential stability. The addition of TCNQ and polarization of the SC-ISE resulted in an enhancement of the potential stability, reducing the drift from −1.4 mV h^{-1} to −0.1 mV h^{-1}, which is the smallest drift recorded with POT-based SC-ISEs. The anticipated outcome is attributed to the TCNQ/$TCNQ^{\bullet-}$ redox couple having a more clearly defined redox potential compared to POT. The inclusion of this redox couple is expected to provide better potential buffering efficiency.[168]

Ali *et al.* developed a miniature sensor for soil NO_3^- determination using nanocomposite composed of POT and molybdenum disulphide (POT–MoS_2) as the ion-to-electron transducer layer (Fig. 13c). Introducing MoS_2 to the POT chain enhances both conductivity and anion exchange, while reducing the formation of a thin water layer at the interface between the electrode and the ISM (Fig. 13d). The sensitivity of NO_3^- detection of the POT–MoS_2 nanocomposite was 64 mV per decade, while POT and MoS_2 alone showed sensitivities of 48 mV per decade and 38 mV per decade, respectively. This suggests that the POT–MoS_2 nanocomposite as SC layer demonstrates improved sensing performances.[166]

During the process of sensor fabrication, there is a propensity for POT layers to dissolve spontaneously and without proper control in the solvent of the ISM cocktail, leading to complications in achieving optimal sensor performance.[116] As an effective strategy for this, Kaluza *et al.* introduced a well-established transducer material and developed a K^+-SC-ISE with good

performance including high potential stability. The SC was created by developing a nanocomposite consisting of multi-walled carbon nanotubes (MWCNTs) and POT. In the composite, POT functions as a dispersing agent for MWCNTs, eliminating the need for a surfactant typically used to stabilize the dispersion of MWCNTs. The composite material derived from MWCNTs and POT overcomes the limitations associated with using MWCNTs and POT individually as SC materials. It effectively prevented the undesired spontaneous transfer of POT into the membrane phase (Fig. 14a) that leads to depletion of the transducer layer and membrane adhesion issues, resulting in the elimination of any potential risk of sensor performance that can occur due to uncontrolled variations in the membrane composition. This happens due to the interactions between MWCNTs and POT which caused to oxidation of POT by MWCNTs serving as the dopants. As a consequence, the polymer becomes immobilized on the carbon nanostructures. The resulting composite exhibits excellent conductivity and a high water contact angle of ~130°, which are essential attributes for a transducer material.[169]

Lenar *et al.* developed a novel ternary composite material comprising three distinct components: carbon nanomaterial (carbon nanotubes and/or carbon black), CP (poly(3-octylthiophene-2,5-diyl)), and metal oxide (hydrous iridium dioxide). The combination of these three components resulted in the creation of superhydrophobic materials exhibiting water contact angles of up to 180° leading to improved stability that can be determined by low potential drift values of 43 μV h^{-1} and 79 μV h^{-1}. Moreover, high electrical capacitance (1.5 and 0.9 mF), low resistance (72.9 ± 0.3 kΩ and 23.5 ± 0.2 kΩ) and wide detection range from 10^{-6} to 10^{-1} M of K^+ ions indicate the improved performance due to triple composite SC.[170] The recent study conducted by Lenar *et al.* have demonstrated that SC developed with POT combining hydrous cerium dioxide ($hCeO_2$–POT) exhibited favourable sensing performance compared to intrinsic POT. This improved performance is due to its high electrical capacitance (112 μF) and water contact angle (120°) (Fig. 14b). High potential stability and wide linear range within the wide range of pH values (2.0–11.5) were also observed. The pH insensitivity of CeO_2 owing to its significant oxide-ion conductivity was leveraged in this study. CeO_2 exhibited pH-sensing capabilities with near-Nernstian response across a broad pH range, including highly alkaline solutions.[86] Table 1 compares the performance characteristics of SC-ISEs developed using different FCPs as ion-to-electron transducers. According to Table 1, the reported sensitivity values are less than 100 mV per decade. The potential drift values reported vary, with the lowest recorded at 1.29 μV h^{-1} (31 μV per day) and the highest exceeding 10^6 μV h^{-1}. Further, the E° standard deviation values span from 0.14 mV to 211.4 mV.

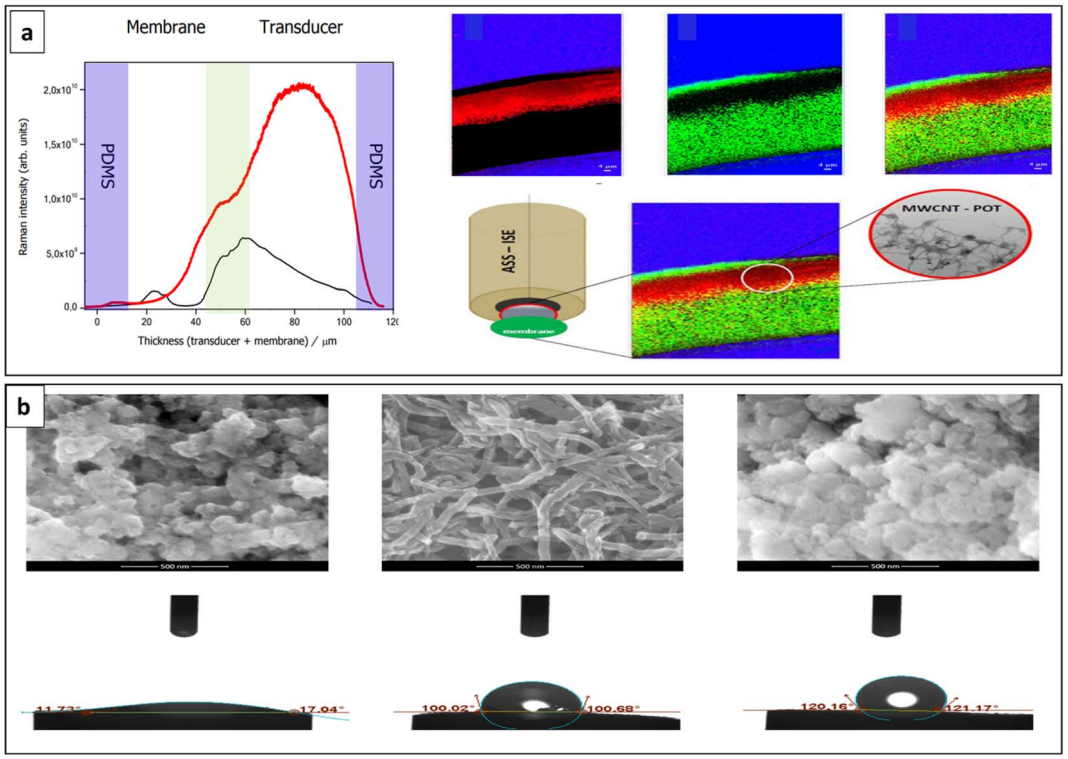

Fig. 14 (a) Emission profiles (left) comparing POT–MWCNTs composite transducer (red line) and POT transducer (black line) and Raman fluorescence maps (right) of the cross-section of ISM and the nanocomposite POT-MWCNTs transducer layer within a PDMS matrix. PDMS, Raman signals of oxidized POT with MWCNT layer and fluorescence of neutral POT are depicted by blue, red and green colored areas, respectively. Reproduced with permission.[169] Copyright 2019, American Chemical Society. (b) SEM images and water contact angles of different materials studied as SCs. Hydrous CeO_2, hydrous CeO_2–CNTs and POT–hydrous CeO_2 (from left to right). Reproduced with permission.[86] Copyright 2022, MDPI, Basel, Switzerland.

Table 1 Comparison of performance characteristics of ISEs with different FCPs as SCs

SC material	Analyte	E° standard deviation	Potential drift	Detection limit	Sensitivity	Linear range	Remarks	Ref.
PPy/zeolite composites	K^+	5.7–17.6 mV	130–180 mV h^{-1}	$\sim10^{-6}$ M	$\sim$53.0 mV per decade	10^{-2}–10^{-6} M	Absence of aqueous layer formation between the SC and ISM	26
PPy–carbon black composite	Tannic acid	—	—	—	17.997 mV per decade	—	No evidence of a water layer formation between SC and ISM Insensitivity to O_2 and light	126
PPy-PFOS	K^+	0.7 mV	69 μV h^{-1}	$(8.8 \pm 2.1) \times 10^{-8}$ M	57.0 ± 0.1 mV per decade	Up to 0.1 M	Water contact angle of 97 ± 5°	91
PPy-MWCNTs	Ag^+	—	—	9.3×10^{-8} M	59.4 ± 0.5 mV per decade	10^{-7}–10^{-1} M	Short response time of about 8 s A Minimum of 50 days of use pH range of 1.6–7.7	120
PANI NFs-Cl^- and PANI NFs-NO_3^-	NO_3^-	0.33 mV for PANI NFs-Cl^-, 0.14 mV for PANI NFs-NO_3^-	0.53 mV h^{-1} for PANI NFs-Cl, 0.84 mV h^{-1} for PANI NFs-NO_3^-	$\sim10^{-6}$ M	$\sim$57 mV per decade	10^{-6}–10^{-1} M	pH range (4.0–12.5) Stable under variable lighting conditions and the presence of gases (O_2)	53
Electrospun PANI microfibers (s-PANI)	Pb^{2+}	—	11.8 μV s^{-1}	6.3×10^{-10} M	28.4 mV per decade	10^{-9}–10^{-3} M	Response time <10 s Validated results with atomic absorption spectrophotometer (AAS)	132
P-NPEDMA-DBS	Ca^{2+}	1.9 mV	—	3.2×10^{-6} M	30.2 ± 0.5 mV per pCa	10^{-7}–10^{-2} M	Absence of pH sensitivity within the pH range of 4 to 9	133
e-PANI-PS or e-PANI microfiber	Pb^{2+}	—	12.3 μV s^{-1}	5×10^{-9} M	29.1 mV per decade	10^{-8}–10^{-3} M	Water contact angle of 104° Fast response time (<10 s) Validated results with AAS	134
PANI-TiO_2	Pb^{2+}	—	122.6 μV s^{-1}	$\sim10^{-9.1}$ M	29 ± 0.2 mV per decade	10^{-3}–10^{-9} M	Response time of 10–15 s High capacitance	135
AgNPs-PANI	Pb^{2+}	—	—	6.31×10^{-10} M	29.1 ± 0.3 mV per decade	10^{-3}–10^{-9} M	High capacitance Response time (<5 s) Real samples analysis with a recovery of 97–109%	136
PANI-graphene	Ca^{2+}	~10 mV	0.2 mV h^{-1}	5×10^{-8} M	28.7 ± 0.1 mV per decade	3×10^{-7}–10^{-4} M	Higher hydrophobicity	51
PANI NFs-Cl:MWCNTs	Cl^-	≤6.1 mV	~0.03 mV h^{-1}	2.56×10^{-6} M	−61.3 mV per decade	5×10^{-6}–10^{-1} M	Response time <10 s pH range 4–9	76
PANI-DNNSA	K^+	4.4 mV	~−0.4 mV h^{-1}	2.5×10^{-6} M	56.9 ± 0.1 mV pK^{-1}	10^{-9}–10^{-1} M	High selectivity against Na^+, Li^+, H^+, Mg^{2+} and Ca^{2+} Insensitive to pH changes within the range of 2 to 7	146
PANI-PFOA	NH_4^+	0.96 mV	13.6 ± 3.2 μV h^{-1}	—	58.07 mV per decade	10^{-5}–10^{-1} M	Superhydrophobicity High resistance to other ions, pH, and CO_2	148
TiO_2–CuO bimetallic/PANI nanocomposite	Vildagliptin	—	—	4.5×10^{-9} M	60.04 ± 1.4 mV per decade	10^{-2}–10^{-8} M	Response time of 10 s ± 1.3	149

Table 1 (*Contd.*)

SC material	Analyte	E° standard deviation	Potential drift	Detection limit	Sensitivity	Linear range	Remarks	Ref.
PEDOTF-TFAB	K^+	0.5 mV (before ISM deposition), 3.0 mV (after ISM deposition)	~50 μV h^{-1}	~3 × 10^{-7} M	58.1 ± 0.6 mV pK^{-1}	—	Water contact angle of 133° Light, O_2 and CO_2 insensitivity	117
PPy-*b*-PCaprol	H^+	8.1 mV	2.5 × 10^{-5} V s^{-1}	—	52.3 ± 0.12 mV per pH	2–7 pH	Redox capacitance of 39.2 μF	38
Graphene/ PEDOT:PSS ink	H^+	98.8 mV	3.8 × 10^{-5} V s^{-1}	—	54.5 ± 7.4 mV per pH	3.5–7 pH	—	38
Meth-PEDOT	H^+	19.4 mV	3.0 × 10^{-4} V s^{-1}	—	53.0 ± 1.7 mV per pH	3–7 pH	—	38
PEI + PEDOT:PSS	H^+	38.5 mV	3.0 × 10^{-4} V s^{-1}	—	49.4 ± 2.0 mV per pH	2–8.5 pH	—	38
PEDOT:PEG	H^+	37.2 mV	1.8 × 10^{-5} V s^{-1}	—	53.9 ± 1.2 mV per pH	3–8 pH	Suitable for mass production of single-used SC-ISEs Redox capacitance of 54.6 μF	38
PEDOT:PSS high conductivity	H^+	211.4 mV	2.2 × 10^{-5} V s^{-1}	—	51.3 ± 7.4 mV per pH	3–7 pH	Redox capacitance of 44.8 μF	38
PEDOT:PEG as a solution-printable SC	NO_3^-	—	—	—	−55.8 mV per decade	0.1 M–1.12 μM	Sustained excellent Hofmeister selectivity with extended continuous use	156
PEDOT-C_{14}(TPFPhB)	H^+	3.7–10.6 mV	~31 μV per day	—	57–58 mV per pH	—	Insensitivity to CO_2 Water contact angle of 136° ± 5° Identical response slopes obtained in the 3–11 pH range	157
PEDOT(PSS) films with 750 nm diameter interconnected pores	Ag^+	3.9–5.4 mV	10.9 ± 2.3 mV s^{-1}	~$10^{-6.5}$ M	56.8 ± 0.4 mV per decade	—	~7 times larger capacitance than compact counterparts Capability to stabilize E° by filling template voids with a redox couple	158
PEDOT-HQ	K^+	2.8 mV	~0.1 mV h^{-1}	~2 × 10^{-7} M	60.9 ± 0.1 mV pK^{-1}	—	Insensitivity to light, O_2 and CO_2 The inner electrode interfaces likely contain water due to the hydrophilic nature of the HQ pendant groups	127
RuO_2-PEDOT:PSS	K^+	0.5 mV	0.077 mV h^{-1}	—	58.93 ± 0.49 mV per decade	10^{-1}–10^{-6} M	Insensitivity to light and pH	153
PEDOT:PEDOT-S	Ca^{2+} and K^+	—	—	0.45 ± 0.01 mM (for Ca^{2+}) 1.68 ± 0.18 μM (For K^+)	28.5 ± 0.3 mV per log[Ca^{2+}] 57.2 ± 0.2 mV per log [K^+]	—	Calibration-free ISEs	154

Table 1 (*Contd.*)

SC material	Analyte	E° standard deviation	Potential drift	Detection limit	Sensitivity	Linear range	Remarks	Ref.
P(EDOTF-EDOT-TEMPO)	K^+	1.84 mV	0.15 mV h^{-1}	$\sim 5 \times 10^{-7}$ M	—	10^{-6}–10^{-1} M	Water contact angle of >130° Insensitivity to light, O_2, and CO_2	34
POT–carbon black nanocomposite	K^+	—	10.9 ± 0.5 μV s^{-1}	$10^{-6.2}$ M	57.6 mV per dacade	10^{-6}–10^{-1} M	Water contact angle of 139.7° Insensitivity to light, O_2 and CO_2	72
POT–RuO_2 nanocomposite	K^+	1.5 mV	86 ± 2 μV s^{-1}	$10^{-6.9}$ M	58.64 ± 0.07 mV per pH	10^{-1}–10^{-6} M	Water contact angle of 149° Electrical capacitance of 1.17 mF Insensitivity to pH, light, CO_2, and O_2	165
POT–TCNQ/$TCNQ^{\bullet -}$	K^+	6 mV	−0.1 mV h^{-1}	—	—	—	Improved potential reproducibility across sensors	168
POT–MoS_2 nanocomposite	NO_3^-	—	95 μV s^{-1}	1.3 ppm	64 mV per decade	Test range from 1 to 1500 ppm	Miniature sensor Developed for soil nitrate determination	166
POT-MWCNTs	K^+	2.9 mV	—	$10^{-6.8}$ M	56.3 ± 0.4 mV per decade	10^{-6}–10^{-1} M	Water contact angle of ∼130°	169
POT–carbon material (carbon nanotubes/carbon black)-hydrous iridium dioxide	K^+	—	43 μV h^{-1} (for carbon nanotubes) 79 μV h^{-1} (for carbon black)	—	—	Test range from 10^{-6} to 10^{-1} M	Water contact angle value up to 180° Electrical capacitance (1.5 mF for carbon nanotubes and 0.9 mF for carbon black) Resistance (72.9 ± 0.3 kΩ for carbon nanotubes and 23.5 ± 0.2 kΩ for carbon black)	170
$hCeO_2$–POT	K^+	0.4 mV	2700 ± 20 μV s^{-1}	—	58.21 ± 0.11 mV per decade	10^{-1}–10^{-6} M	Electrical capacitance of 112 μF Water contact angle of 120° Potential stability within the pH range of 2.0–11.5	86

6. Ion-selective membranes

6.1 ISM composition and mechanism of selective sensing

For several decades, ISEs with solvent-polymeric membranes, comprising neutral and charged ionophores, have served as potentiometric sensors for quantifying a broad spectrum of analytes.[114,171–173] The ISMs employed in potentiometric sensors are composed of several essential constituents blended in a meticulously balanced ratio.[174] An ISM generally consists of an ionophore, ion exchanger, and a polymer matrix which may include a plasticizer.[41] In ISEs, the transducer undergoes a redox process triggered by an electrochemical stimulus, resulting in ion exchange with the ISM, ion transportation within the phase, and ion exchange at the interface between the ISM and the sample.[175] ISM immobilized with lipophilic organic anion (ionophore) as the ion receptor undergoes selective binding with the target ion[6,176] through chemisorption and achieves an equilibrium potential that changes in a logarithmic manner depending on the concentration of the target ion in the electrolyte.[6] Further, ISMs are incorporated with additives and plasticizers. Additives enhance the membrane selectivity and reduce electrical resistance. Moreover, plasticizers are employed to facilitate the attachment of the ionophore and additives onto the electrode surface.[177] The presence of a highly selective ionophore in the ISM enables the measurement of the concentration of specific free ions of interest, even in the presence of other chemical forms of the analyte that may potentially interfere, within complex matrices.[174,178,179] To ensure stable sensor performance, the primary ions are incorporated into the ISM during the pre-treatment step.[174] Analyte ions in the ISM phase preferentially undergo ion exchange with the ISM due to their complexation with the ionophore.[41,174] Furthermore, the thickness of the ISM influences certain factors regarding ISEs such as the applied technique of analysis and conditioning prior to use.[180]

The ISM's composition influences ion diffusion rate through the receptor response pattern,[181–184] electrical conductivity,[185] and practical usability.[8] To maintain a consistent ISM composition, certain conditions must be fulfilled: the membrane needs ion-exchanger properties, sufficient hydrophobicity to prevent significant coextraction of counterions, absence of electrically neutral interfering species causing emf shift, presence of a selective lipophilic ligand/ionophore for the target analyte ion, and avoiding excessive binding of the ligand to the analyte ion to preserve membrane permselectivity.[41] The properties of the ISMs largely dictate the analytical performance of the sensor, including factors such as the sensitivity, linear range of response, and selectivity.[3,41] Alterations in the composition of the ISM, both in terms of its qualitative and quantitative aspects, have an impact on the analytical functionality of sensors.[174] Potentiometric ISEs are user-friendly, durable, energy-efficient devices that offer good selectivity and sensitivity. They can be seamlessly integrated with communication devices. In order to explore different ways of obtaining data and obtaining additional information about species, ISEs have been investigated using chronoamperometry, chronopotentiometry, thin layer coulometry, and cyclic voltammetry. In several of these methods, the composition and material of the ISM need to be adjusted appropriately to support the currents involved.[22]

6.2 Drawbacks of conventional ISMs

Achieving optimal analytical performance of the membrane is commonly acknowledged to rely on precisely defining the composition of the phase through the deliberate addition of specific components during preparation.[174] Polymeric ISMs have been extensively researched and employed in ISEs for approximately five decades.[186] The majority of ISMs were plastic films that produced through the process of drop casting the ISM cocktail containing dissolved ionophores and polyvinyl chloride (PVC) onto the transducer layer and evaporating the solvent.[56,174,187] PVC stands as the most frequently employed polymer matrix in SS-ISEs. Nevertheless, there are certain limitations associated with this kind of ISM.[177] For instance, when the PVC content was reduced, the ISM became thin and prone to cracking.[56] Nonetheless, the adhesion of PVC to the transducer surface is generally unsatisfactory due to the reliance on weak van der Waals interactions for membrane immobilization. Ensuring a robust attachment of the membrane to the sensor surface is vital, as a weak connection can result in significant issues concerning response stability and reproducibility. The fragmentation or leaching of membrane compounds can lead to a reduced lifespan of the sensor and a loss of its functional capabilities.[177] The infiltration of water through the membrane is a leading factor contributing to sensor failures in this type of ISE. The absorption of water leads to the formation of thin aqueous layers or pools at the electrode interfaces, causing potential instability and inadequate adhesion of the membrane to the SC.[133] Additionally, the ISM exhibits poor conductivity, which negatively impacts the efficiency of ion transmission.[56] It is crucial for the ISMs to exhibit chemical stability, inertness, low electrical resistance, biocompatibility, and non-toxicity.[177] Therefore, there remains a strong demand for the development of stable ASS-ISEs, which necessitates the exploration of new materials and technologies for ISMs.

6.3 Application of FCPs and CP-based systems in ISMs

The emphasis on using CPs for potentiometric sensors was due to their potential as alternative membranes to traditional ISMs.[77,164] However, CPs considered to be unsuitable for potentiometric sensors when employed as exclusive substitute membrane materials, such as for plastic polymeric materials. This is primarily because CP membranes encounter interference from redox reactants in the solution,[188] variations in sample pH,[189,190] and inadequate ionic selectivity.[45,191] Nevertheless, recent studies have shown that integrating CPs into ISMs and utilizing state-of-art technologies, improve the analytical properties, such as high sensitivity,[175] low detection limits, and absence of detected redox sensitivity.[192] CP-based membranes belong to a novel category of advanced materials that find utility in separating or facilitating the interphase

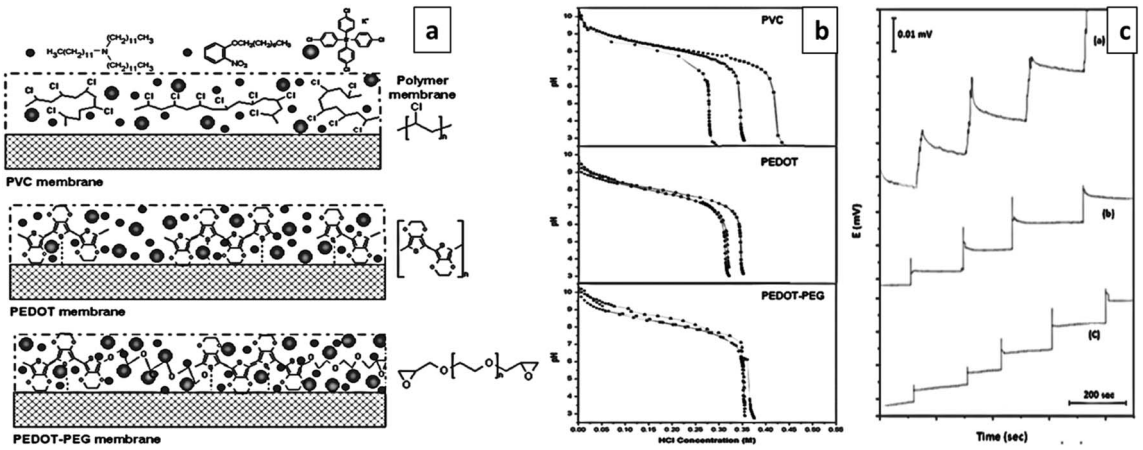

Fig. 15 (a) Diagram outlining the ISMs (PVC, PEDOT and PEDOT-PEG), (b) repetition of the response and (c) comparison of kinetic responses. Reproduced with permission.[177] Copyright 2014, MDPI, Basel, Switzerland.

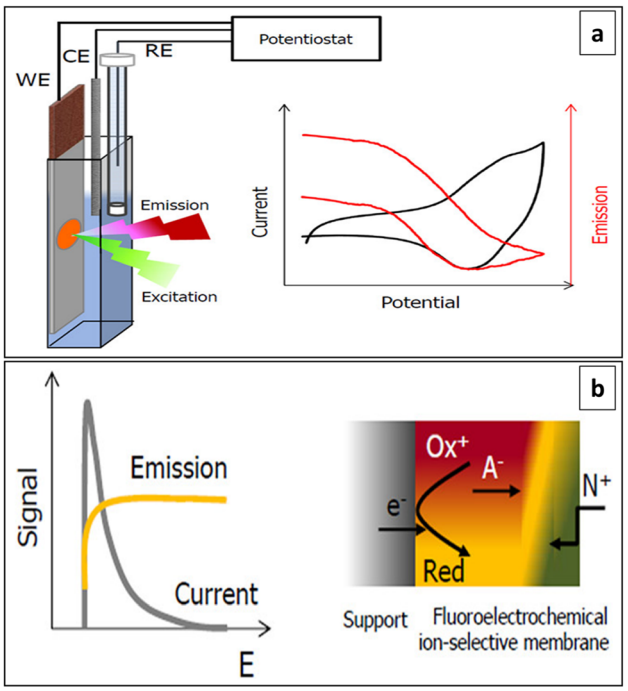

Fig. 16 (a) *In situ* transduction of electrochemical responses to emission change signal of ISEs operating under non-zero-current conditions. (b) Schematic representation of the mechanism of fluoroelectrochemical ISMs. Reproduced with permission.[175] Copyright 2021, American Chemical Society.

transfer of specific chemical species by leveraging their electrical properties.[88]

To address the challenges associated with PVC membranes, Mir *et al.* introduced two sensor platforms for pH sensing. Both sensor configurations were established by electropolymerizing PEDOT on the electrode surface and incorporating the ionophore and additives within the polymer matrix. PEDOT, containing sulfur groups, forms a robust dative binding with the gold surface, resulting in a highly stable conformation that hinders membrane leaching and degradation. In the second developed configuration, a crosslinker, poly(ethylene glycol) diglycidyl ether (PEG), was introduced to PEDOT at a specific concentration (Fig. 15a). The inclusion of a PEG layer brings additional benefits such as flexibility and biocompatibility. The resultant ISMs exhibited improved stabilization of the sensor response in comparison with the PVC matrix, along with enhanced reproducibility and stability (Fig. 15b and c).[177]

Electropolymerization offers numerous advantages for depositing selective layers in the fabrication of chemical sensors.[193] Polymerization of PPy in electrolytes with various counter ions allows easy modification of the polymer's functionality and properties.[194] PPy exists in a neutral reduced state and a positive oxidized state. However, during synthesis, it is possible to produce anion-sensitive and cation-sensitive films by using small inorganic anions or large organic anions as counter ions.[195] PPy is electroactive and functions as an ion exchanger during redox reactions. When undergoing charging and discharging (doping–dedoping) processes, PPy exchanges ions based on the dopant's size and the applied potential on the membrane.[196] Using these properties of PPy, Zhang *et al.* presented a new approach to fabricating sensitive membranes through the "molecularly imprinted" technology for specific ion recognition. This technique enables the membranes to selectively identify and interact with the desired target ions, offering a novel method in their preparation. An ASS-ISE for NO_3^- ions by molecular imprinted NO_3^--doped PPy polymer layer was developed. During the electrochemical process of p-doping polymerization using pyrrole monomer, it is necessary for the positive charge within the resulting polymer structure to interact with a negative charge, ensuring electrical neutrality. To achieve this, NO_3^- with its negative charge is introduced and doped into the PPy molecular chain during polymerization, creating a specific physical space "molecularly imprinted key" for the specific recognition of NO_3^-. Here, the process of electrodeposition was utilized to produce a high-performance PPy-NO_3^- membrane. The research findings indicate that the newly developed ASS-ISE exhibits exceptional selectivity towards NO_3^-

ions, and its performance remains unaffected by the presence of Cl^-, Br^-, SO_4^{2-}, or PO_4^{3-} ions.[56] The fundamental innovation in this research arises from the distinctive properties of PPy. During electropolymerization, anions from the reaction solution can be integrated into the polymer as dopants or counterions. These incorporated anions, known as dopants, impart their properties to the polymer product. The characteristics and general properties of PPy CPs are determined by the polymer dopant anions.[49] Recently, Gao *et al.* also reported a NO_3^--SC-ISE using NO_3^--doped PPy ISM. The study revealed that the roughest NO_3^--doped PPy ISM significantly enhances the effective contact surface area of ISM with NO_3^- solution. This results in improved NO_3^- ion adsorption on the NO_3^--doped PPy ISM, leading to a higher electron generation with a potential response of Nernstian slope of 54.0 mV per decade and LOD of 1.1×10^{-4} M.[197]

In recent times, the utilization of composite materials as ISMs has garnered considerable attention from researchers. Moreover, there has been a growing interest among scientists in "spectroelectrochemistry" that involves combining the optical readout with an electrochemical trigger under non-zero-current conditions for ion sensing, leading to the development of opto-electro dual sensing systems (photoelectrochemical sensors). For this approach, redox and optical active CPs such as POT are used in ISM preparation. In this regard, Wegrzyn *et al.* used composite materials as ISMs and introduced a new type of fluoroelectrochemical composite ISM that includes ionophore, cation-exchanger and a dispersed CP that serves as an ion-to-electron transducer capable of both redox and emission activity embedded in a plasticized PVC matrix as a single layer (Fig. 16a). This enables the *in situ* conversion of electrochemical response to emission change signals, operating under non-zero-current conditions. Here, K^+-selective sensors were examined as a model system for emission readout ISEs, with POT being utilized as the CP. The application of an electrochemical trigger initiates a redox process in the POT, leading to ion exchange between the ISM and the solution. This exchange subsequently causes a change in the emission spectrum of the POT (Fig. 16b). The emission intensity changes are correlated with the electrochemical responses observed when operating under non-zero-current conditions, resulting in low detection limits and wide linear response ranges when operating in coulometric conditions. There are several reasons for using a composite material as a membrane.[175] The utilization of a composite material as an ISM results in an increased contact area between the CP and ISM, which has been demonstrated to be crucial for sensors operating under coulometric conditions.[23,175] Moreover, this approach enables precise control over the membrane composition, including the ability to manage the effects associated with interactions between CP and the ionophore/ion exchanger,[175,198] achieved by eliminating the spontaneous migration of CP into the membrane phase.[116,175] The proposed optical readout mode addresses challenges related to the high resistance of ISMs in non-zero-current methods. It enables higher sensitivity and extends the linear response range.[175]

Conventionally, CPs are utilized in ISMs under zero-current potentiometric/open circuit potentiometric conditions.[192,199] This involves the reversible ion-to-electron transfer at the rear of the ISM.[192] Although advanced electrochemical sensing technology can provide sufficient selectivity and sensitivity,[200,201] it relies on conventional transduction principles like potentiometry and amperometry. However, these principles were not designed for recalibration-free and robust sensing applications.[200] Earlier, the non-zero current mode of measuring with ISEs was primarily focused on studying the electrode response mechanism, selectivity origins,[171,202,203] and enhancing the detection limits[115,171,204] and sensitivity, especially for polyion sensing.[85,205–207] Analytical applications of ISEs in the non-zero current mode were rare until 2010. However, in recent years, the practical usage of ISEs employing techniques such as voltammetry, amperometry, coulometry, and chronopotentiometry has become prevalent.[171] The increasing interest in electrochemically triggered ion-selective sensing under non-zero current conditions motivates the search for alternative constructions and membrane compositions for probes suitable in this sensing scenario.[192] In electrochemically triggered applications, the transducer becomes active by undergoing a redox process induced by the applied potential/current. This leads to ion exchange with the ISM, ion transport within the phase and ion exchange at the interface between the ISM and the sample.[192] The typical approach for ASS-ISEs involves the use of an ion-to-electron transducer that is covered with a classical ISM that experiences significant ohmic resistance of ISE system.[192] In current-triggered approaches, this factor can be disadvantageous, but it is usually overcome by using thin ISMs. However, employing thin membranes raises the risk of membrane fragility and unintended spontaneous composition changes.[116,174,192,208]

Then this structure evolved into a unified phase with a mixture of ISM insoluble CP particulates. It creates a heterogeneous system in the ISM,[192] encompassing drawbacks such as issues associated with the direct casting of ISM cocktail onto the substrate without CPs,[54,61] redox sensitivity[54,61] related to the CP particulates directly in contact with the solution[209] particularly at higher CP loadings and relatively high detection limits.[54,61] Recently, there has been a growing interest in the concept of single-piece sensors that involve single-piece membranes prepared using composite materials that incorporate CPs within a plasticizer matrix as ISM to achieve improved sensing characteristics.[175,192] A soluble CP is mixed with an ISM cocktail that includes the usual components found in a traditional PVC matrix membrane and is directly applied onto a solid substrate. The CP acts as a mediator for charge transfer between the substrate and the membrane.[61] Using the transducer as a dispersion in membrane plasticizer enables the system to be utilized under electrochemically triggered conditions and has several advantages, including simplified membrane preparation and reduced risks associated with particulate formation and their random distribution within the ISM. Furthermore, significant improvements were also made in the potentiometric mode with an ISM containing dispersed CP. These include the detection limit shifted to typical values, and no observed redox sensitivity.[192] The current-triggered sensing mode provides distinct advantages, encompassing low detection limits, high sensitivity, and the ability to reduce the frequency of calibration.[192]

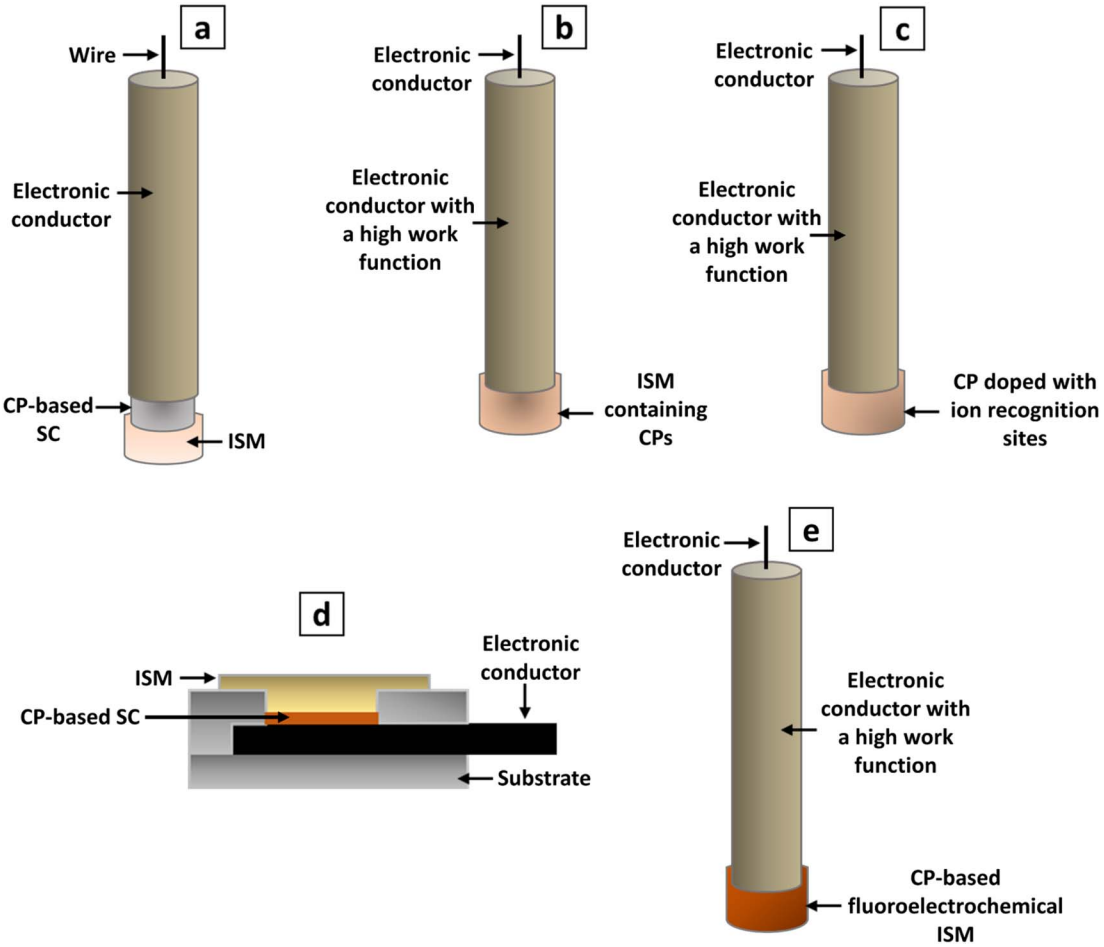

Fig. 17 Different types of CP-based ISEs. (a) ASS-ISE with CP-based transducer, (b) single-piece ISE, (c) ISEs with CP-based ISMs, (d) miniaturized ASS-ISEs with CP-based transducers and (e) ISEs with dual sensing systems; electrochemical and emission signals.

Jaworska *et al.* proposed an alternative to traditional ISEs in current-triggered electrochemical sensing. Their proposal involved using an ISM with a dispersed CP, as a successful alternative to the typical approach that utilizes a CP layer covered with an ISM.[192] Thus, FCPs were incorporated into plasticized PVC-based ISMs. This integration allows the CP to potentially affect the sensor's selectivity, depending on the concentration of the CP within the ISM.[77] The resulting system obtained from this approach eliminates a critical weakness commonly found in heterogeneous ISM, which is the presence of solid particulates dispersed within the polymeric ISM. The single-piece ISE concept was studied using K^+-ISEs as the model sensors, incorporating the CP, poly(3-hexylthiophene) (PHT), which is highly soluble in a typical PVC-based membrane plasticizer. It has been observed that the inclusion of PHT in the ISM composition primarily impacts the resistance of the ISM. Under voltammetric conditions, this leads to a decrease in the cathodic peak potentials for high PHT contents. Consequently, as the PHT content increases, the slope of the cathodic peak potential dependence on the logarithm of analyte concentration rises from the Nernstian value to *ca.* 100 mV per decade which is an indicative of preserved linear correlation between these two variables. Additionally, higher PHT contents result in significantly higher recorded currents and demonstrated appealing performance in both open circuit and electrochemically triggered modes.[192] Fig. 17 shows the type of CP-based ASS-ISEs.

7. Ion-selective optodes

7.1 Basic structure and mechanism of sensing

The increasing needs for chemical analysis in environmental, biological, clinical, and food chemistry have led to significant interest in the development of ion-selective optical sensors.[210] Optodes are based on two principles[211] that cation sensing relies on ion exchange, while anion measurement typically utilizes co-extraction.[14,212] Optodes, being ISSs, investigate ion-exchange[213,214] or co-extraction[211,214] at the interface to observe the binding of analyte ions to a neutral ionophore within the probe's bulk.[213] ISOs provide a promising opportunity for highly selective optical detection of ions by utilizing optically silent ionophores in conjunction with optical transducers.[215] Film-based ion optodes find applications in fiber optics, flow cells, and waveguide devices.[40] Generally, an ISO consists of several components. A lipophilic medium, typically plasticized

poly(vinyl chloride)[7,216,217] or polyacrylate polymer, that is inert.[7,216] It contains an ion-exchanger,[218] a probe-ionophore that detects the analyte,[7,216,218,219] along with an H^+ ionophore[7,216] usually a pH-sensitive dye that is relatively lipophilic[220,221] and has varying optical properties when protonated or deprotonated. The H^+ ionophore is used as the optical transducer.[7,216] This combination enables the optical measurement of changes in analyte concentrations within a sample.[222] In a typical cation-sensitive system, the operational principle relies on the competition between H^+ ions and the analyte cation for binding in the lipophilic phase.[221,223,224] The analyte's binding causes the dye to deprotonate, ensuring the probe remains electrically neutral. This deprotonation is observed as a measurable alteration in the optical spectra of the transducer (turn-on mechanism).[213] In a typical anion-sensitive system, a change in color or fluorescence signal results from the protonation of the chromoionophore due to the co-extraction of the target anion and a proton from the aqueous sample into the organic phase.[225]

Except the classical H^+ sensitive chromoionophores, various optical transducers have been used[226–228] such as CPs, solvatochromic dyes, and other charged dyes with aggregation-induced emission or aggregation-caused quenching.[14] Optical detection of ion concentration is appealing due to its simplicity, making it suitable for handheld and zero-power devices.[22] ISOs predominantly function as bulk sensors.[229] The analytical signal of optodes typically follows a sigmoidal pattern that depends on the logarithm of the analyte concentration, spanning a range of 2–3 orders of magnitude.[9] ISOs have the capability to be miniaturized, reaching nanoscale dimensions. They find utility in bioanalytical applications and the mapping of ion gradients.[40,210] Optodes offer both advantages and disadvantages in comparison to other ion-selective technologies like ISEs.[219] Generally, optodes are low cost, suitable for on-line applications, and have low mass and power requirements.[219,230] The reading signal of ISOs is easily achieved, even without the need for complex instrumentation or reference electrodes.[9] Regardless of the format used, ISOs are typically not pre-treated prior to their use.[231] However, they are limited to single-component detection and have received less attention.[219]

7.2 FCP-based optical transducers

Since the majority of ionophores do not exhibit optical activity, the optode composition necessitates the inclusion of an optical transducer, such as a pH-sensitive dye, to enable optical detection.[232] When the analyte binds to the ionophore in the probe, the dye within the probe undergoes deprotonation to maintain probe electroneutrality, assuming a constant sample pH.[229] A major drawback of this approach is the optical transducer's susceptibility to cross sensitivity caused by changes in the pH of the sample.[213] A common issue with many optodes that use H^+ selective ionophore as optical transducer is their gradual bleaching,[233,234] which refers to a decrease in the optical signal over time. This can occur due to the spontaneous transfer of the deprotonated form of the dye from the lipophilic phase to the aqueous solution,[234] leading to a reduction in emission intensity.[220,234] The alternative approach of using polarity-sensitive dyes as optical transducers often leads to a decrease in emission response as the analyte concentration increases. However, this characteristic can be disadvantageous in certain applications.[235]

As an excellent alternative, CPs such as polyalkylthiophenes have been widely employed as optical transducers due to several reasons.[236] CPs possess a conjugated structure and sufficiently low electronic band gap, enabling them to absorb electromagnetic radiation across ultraviolet, visible, and even near-infrared regions, thereby producing colored compounds. Adjustment of the dopant and doping level of CPs, either chemically or electrochemically, leads to a remarkable and dynamic alteration in their optical properties.[46] CPs, such as polythiophenes, are regarded as significant optoelectronic materials. These materials exhibit changes in their absorption and emission properties, which are attributed to the presence of delocalized π electrons.[237] When the analyte binds to the probe, it causes a transformation of the positively charged polymer backbones into neutral, semiconducting, and optically active forms, without involving a redox reaction with the solution. This adjustment leads to an amplified optical signal as the analyte concentration increases and provides the benefit of reduced dependence on the pH of the sample.[198,222,238,239] The change in the polymer's oxidation state necessitates the exchange of ions to maintain the overall electrical neutrality of the CP. When the neutral form of the CP (CP^0) exhibits fluorescence while the oxidized form (CP^+) does not, the alteration in the polymer's oxidation state can be detected by observing changes in emission (eqn (1)).[222]

$$\underset{\text{(fluorescent)}}{\left(CP^0X^-N^+\right)_{CP}} \leftrightarrow \underset{\text{(non-fluorescent)}}{\left(CP^+X^-\right)_{CP} + N^+_{solution} + e^-} \quad (1)$$

If ion exchange is impeded, the polymer's redox state remains unaltered, and there will be no discernible change in emission. However, when specific ion exchanges are favoured, such as through selective complexation within the polymer by a neutral ligand, the formation of charged complexes within the polymer matrix disrupts the electrical neutrality of the polymer phase. This disruption can only be rectified by adjusting the quantities of CP^0 and CP^+. Consequently, the binding of the analyte in the nanosphere can be tracked by observing changes in the system's emission (eqn (2)).[222]

$$\underset{\text{(lower fluorescence)}}{\left(nCP^+mCP^0X^-L\right)_{CP} + M^{z+}_{solution}} \leftrightarrow \underset{\text{(higher fluorescence)}}{\left((n-z)CP^+(m+z)CP^0X^-LM^{z+}\right)_{CP}} \quad (2)$$

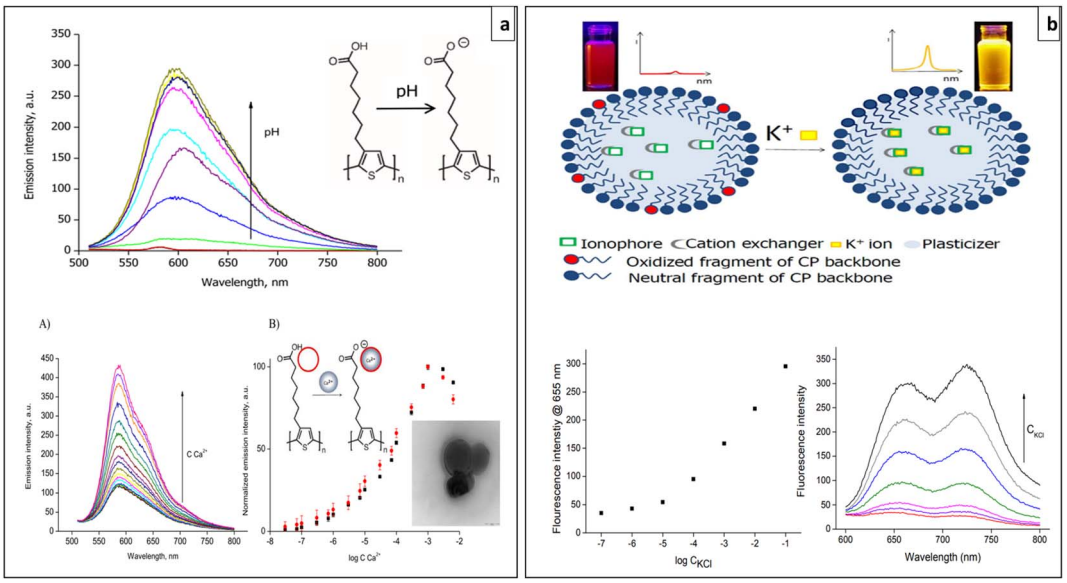

Fig. 18 (a) PHT-COOH nanostructure-based optodes. Emission spectra change with pH and schematic illustration of the transformation to its corresponding polymeric anion (upper) and emission spectra change with increasing Ca^{2+} ions, emission intensity *vs.* logarithm of the concentration of Ca^{2+} ions, schematic illustration of the transformation of PHT-COOH to corresponding polymeric anion and TEM image of Ca-PHT-COOH nanoptodes (lower). Reproduced with permission.[215] Copyright 2020, Elsevier. (b) Schematic illustration of novel optical transduction mechanism proposed using plasticized POT nanospheres loaded with NaTFPB and valinomycin (upper), emission intensity *vs.* logarithm of the concentration of K^+ ions plot and emission spectra with and without K^+ ions (lower). Reproduced with permission.[222] Copyright 2016, American Chemical Society.

For both eqn (1) and (2), where CP^0 and CP^+ are neutral and the oxidized form of the CP respectively, X^- is lipophilic anion, N^+ is a cation, M^{z+} is analyte cation and L is ionophore. Polyalkylthiophenes exhibit bright emission when in a neutral state, but their emission is significantly reduced when they undergo oxidation.[236] In contrast, the emission properties of polythiophenes rely heavily on the arrangement of the polymer chains, specifically the configuration of the chromophore thiophene groups.[240]

Considering aggregation-related effects of PHT optical transducer, to increase the stability of emission signals, Kisiel *et al.* suggested using ion-selective de-aggregation of quenched polymer as an effective transduction mechanism for optodes (Fig. 18a). This mechanism involves alterations in the suspended nanostructural aggregate by incorporating the analyte selectively, which rearranges upon analyte binding and forms stable polymeric micelles altering the spatial arrangement of chromophore groups within the nanostructure, leading to the generation of a bright and highly stable optical signal. The formation of micelles, driven by ion-selective interactions, leads to a significant increase in emission by reducing the quenching caused by aggregation, which is a characteristic of dispersed phase formation. They studied this phenomenon by employing a model system consisting of Ca^{2+} selective optodes. These optodes were created using poly[3-(6-carboxyhexyl)thiophene-2,5-diyl] (PHT-COOH) as an optical transducer and nanoptode matrix. The developed optodes exhibited an emission signal increase across a broad concentration range of analytes, ranging from 10^{-7} to 10^{-3} M. They demonstrated a turn-on response within a wide pH range of 6.3 to 8.9. Importantly, there was no evidence of optical signal degradation after a 5-day exposure to the analyte or during storage for more than two weeks. An important distinction from other known systems is that the change induced by analyte binding does not impact the chromophore group directly. Instead, it takes place at a distant, terminal position of the polymer's side chain.[215]

Klucinska *et al.* introduced a new type of ion-selective nanooptodes that eliminate the need for a pH-sensitive dye, which is commonly required in most proposed optodes. Instead, they use a CP as both the optical transducer and nanoprobe material. POT was studied as optical transducers in prepared K^+ ion selective model optode system and a linear relationship between emission intensity and the logarithm of analyte concentration was displayed across a wide range spanning from 10^{-5} to 0.1 M in the turn-on mode (Fig. 18b). The POT exists in a partially oxidized state, with positive charges that cause its emission to be quenched. The receptor, an optically inactive uncharged ionophore, selectively binds to the K^+ ions. When binding occurs, positive charges are generated within the nanosphere, causing a decrease in the oxidation state of POT without any change in redox potential. This leads to an increase in emission. The emission change is directly influenced by the alteration in the ratio of oxidized to neutral polymer units within the nanoparticle. The linear response over a wide concentration range of analyte is attributed to the novel optical transduction mechanism and high lipophilicity of the polymer matrix.[222]

Stelmach *et al.* reported POT nanospheres-based nanoptodes for K^+ and Ca^{2+} ions that operate in a turn-on mode without involving hydrogen ion exchange, thus eliminating the pH

sensitivity commonly seen in classical ISOs that use pH sensitive dyes as transducers. The research discovered that the redox potential of the solution, influenced by solution pH and oxygen levels, affects the oxidation state of the polymer and subsequently impacts the sensor's performance. They developed poly(3-octylthiophene-2,5-diyl)-sodium tetraphenylborate-valinomycin (POT-NaTFPB-Val) as K^+-ISOs, and poly(3-octylthiophene-2,5-diyl)-sodium tetraphenylborate-ETH 1001 calcium selective ionophore (POT-NaTFPB-ETH 1001) as Ca^{2+}-ISOs. By adjusting the composition of POT optodes and incorporating a hydrogen binding compound in the polymer phase, the sensitivity of the optode to pH changes was effectively reduced. The proposed nanoptodes exhibited high sensitivity for emission change in both alkaline (pH = 9.2) and acidic (pH = 4.0) pH ranges. They demonstrated a broad linear dependence of emission intensity on the logarithm of analyte concentration, spanning six orders of magnitude in turn-on mode.[198] However, further modifications are required to eliminate the pH sensitivity at extreme pH levels.

8. Conclusions and future perspectives

In the past decade, many significant developments in FCP-based ISSs can be witnessed. The advancements have sparked renewed interest in exploring previously deemed unattainable areas of application. The limitations associated with intrinsic CPs can be addressed by customizing the properties through appropriate functionalization with materials that possess tailored properties.

Synergistic properties of FCPs open a wide window of opportunities in producing outstanding electrode materials with enhanced characteristics, including high redox capacitance, lower resistance, high electrical conductivity, high exchange currents at interfaces, large surface area, and increased hydrophobicity. Stable potentiometric responses can be achieved through several approaches. To enhance E° reproducibility, approaches such as, functionalization with hydrophobic groups, incorporation of lipophilic additives and prepolarization have been employed. Moreover, a variety of carbon-based materials such as graphene, carbon nanotubes and carbon black have been incorporated to enhance E° reproducibility.

Among the various ion-to-electron transducers described in this review, the lowest potential drift of 1.29 μV h^{-1} (31 μV per day) was reported with the superhydrophobic PEDOT-C_{14}-(TPFPhB) SC. The best E° standard deviation reported was 0.14 mV and reported sensitivity values are less than 100 mV per decade. Moreover, another constraint is the undesired spontaneous transfer of the CP transducer into the ISM and it can be effectively prevented by immobilizing the CPs in carbon nanostructures such as MWCNTs which act as dopants.

The commonly encountered shortcomings of PVC-based ISMs such as membrane instability and low selectivity can be effectively addressed by employing FCPs in ISMs. CP composite materials are employed as ISMs to increase the contact area between the CP and ISM and enable precise control over the membrane composition. CPs can be used as dispersions by mixing with ISM cocktail, enabling the utilization of ISEs under electrochemically triggered conditions. Furthermore, there has been a recent upsurge in spectroelectrochemistry that involves fluoroelectrochemical ISMs dispersing both redox and emission active CPs, in a plasticized PVC matrix enabling the *in situ* conversion of electrochemical responses to emission change signals, operating under non-zero-current conditions. These modifications have provided better analytical performances and ultimately led to the development of concepts of opto-electro dual sensing systems (photoelectrochemical sensors) and single-piece sensors. Further, these advancements have led to progress from conventional zero-current potentiometric ion sensing to dynamic innovative integrated sensing approaches.

Recent research have shown that the use of FCP nanoparticles as optical transducers has overcome limitations and led to improved sensing properties (*e.g.*, increased stability of emission signal). Introducing novel optical signal transduction mechanisms such as changing spatial arrangements through selective inclusion of analyte resulted in bright and highly stable optical signals. Further, it has been reported that by incorporating hydrogen binding compounds such as NaTFPB into CPs, pH sensitivity has effectively reduced within a considerable pH range of 4–9.

Despite the impressive properties of some CP-based ISSs and their potential advantages, they have mainly stayed confined to research laboratories due to lack of desired features. Therefore, it is crucial to engineer CPs that can match or even surpass the performance characteristics of existing sensors. There is still room for developing ISSs with enhanced performances. For example, the fabrication of SC-ISEs in configurations suitable for different applications/purposes such as calibration-free, miniaturized, wearable, remote-controlled, autonomous, and field-deployable is very much desired. The main constraint for this is achieving E° reproducibility within single and different batches. Achieving very low levels of E° standard deviation (0.1 mV), potential drift (0.1 μV h^{-1}), and high levels of sensitivity (≥100 mV per decade) is still challenging. Considering ISOs, it remains difficult to achieve pH insensitivity in extreme pH levels (<4 and >9) with CP-based optical transducers.

In the future, FCP-based ion sensing platforms are expected to become highly prevalent and widely used across various industrial sectors, including healthcare, environmental monitoring, pharmaceuticals, and the food and beverage industry over other ion detection techniques. The focus can be expected on achieving real-time and online monitoring of ions, wireless sensors that combine wireless communication technologies (*e.g.*, Bluetooth, NFC) and multi-sensing lab on chips to fabricate sensor devices with multiple operational modes. For example, the future healthcare industry can be strengthened through portable and wearable ISEs for detecting ions non-invasively in biological fluids like sweat as these ions can serve as important biomarkers for continuously and intermittently monitoring health conditions. In this scenario, the ISEs-integrated wearable devices can be developed into watches, tattoos, epidermal patches, *etc.* for more advanced real-time

monitoring. These sensors must have excellent performance over multiple uses without the need to switch electrodes or cleaning between uses.

Despite significant and continuous progress in the field, the process of selecting materials and functionalization methods is still young and rapidly growing. Therefore, extensive research efforts are anticipated in the coming years to advance this aspect further. Improving ISEs/ISOs using FCPs in the future will likely involve a combination of advancements in material design, fabrication techniques, and integration with other technologies to enhance selectivity, sensitivity, stability, and response time. Although materials like transition metals, metal oxides, and carbon nanomaterials have made significant advancements as secondary materials in CP composites, there is a need to prioritize the exploration of emerging new advanced materials like two-dimensional (2D) transition metal carbides and nitrides (MXenes) and 2D transition metal borides (MBenes) which contain excellent electrical and mechanical properties, to functionalize with CPs that are not frequently reported in the literature. It's worth noting that while FCPs like CP-composites and doped CPs, hold great promise for improving ISSs, challenges still remain related to stability, reproducibility, and long-term performance. In this scenario, it can be suggested that, the multiple-composite materials that combine more than two materials that integrate several different properties as promising candidates for ISS materials. This can dramatically increase the ideal ion detection possibilities and resolve the existing bottlenecks regarding multi-analyte sensing, miniaturization, *etc.* However, the studies should be focused on effective synthesizing and functionalization approaches for combining multiple components. In addition, designing FCPs that can withstand various environmental conditions makes the ISSs versatile for different applications, offering new prospects for space exploration and enabling deployment in extreme environments.

There is a strong demand for extensive research on the use of FCPs in the fabrication of emerging opto-electro dual sensing systems. Their special feature, where signal induction and measurement are performed in two different ways; optically or electrochemically, allows this system to be adapted to measure more than one single ion through strategic adjustments.

ISOs are constantly evolving with the introduction of new and innovative concepts and enhancements to conventional detection modes and a wide range of sensor materials. Although there has been remarkable progress, certain aspects still need significant improvements, such as pH cross-response, emission signal instability, brightness, and photostability of the chromoionophore. The future development of ISOs will depend on the increasing demand for ISOs that possess biocompatibility, self-assembly, real sample measurement without pretreatment and unique analytical performance. Therefore, ISOs are likely to become widely accepted and increasingly used in pragmatic implementations.

There is a great scope for extended research activities in ISSs with FCP materials. Advancements in this field are multifaceted and can significantly enhance the accuracy, sensitivity, and specificity of ion detection, leading to more reliable and efficient systems. Collaborative efforts between material scientists, chemists, engineers, and application specialists are essential to drive these advancements and translate them into practical and real-world applications.

Data availability

All data and information supporting this article have been included within the manuscript.

Conflicts of interest

There are no conflicts of interest to declare.

Acknowledgements

The authors would like to express their gratitude to all the members who have contributed to advancing knowledge in electrodes and related subjects within the Department of Chemistry, University of Colombo, Sri Lanka.

References

1 B. P. Nikolskii and E. A. Materova, *Ion-Sel. Electrode Rev.*, 1985, **7**, 3–39.
2 X. Wang, Y. Qin and M. E. Meyerhoff, *Chem. Commun.*, 2015, **51**, 15176–15179.
3 P. Bühlmann, E. Pretsch and E. Bakker, *Chem. Rev.*, 1998, **98**, 1593–1687.
4 R. N. Liang, D. A. Song, R. M. Zhang and W. Qin, *Angew. Chem., Int. Ed.*, 2010, **49**, 2556–2559.
5 V. Sethumadhavan, S. Rudd, E. Switalska, K. Zuber, P. Teasdale and D. Evans, *BMC Mater.*, 2019, **1**, 1–14.
6 Y. Shao, Y. Ying and J. Ping, *Chem. Soc. Rev.*, 2020, **49**, 4405–4465.
7 M. J. Ruedas-Rama, J. D. Walters, A. Orte and E. A. H. Hall, *Anal. Chim. Acta*, 2012, **751**, 1–23.
8 K. Maksymiuk and A. Michalska, *Curr. Opin. Electrochem.*, 2020, **23**, 74–79.
9 E. Stelmach, K. Maksymiuk and A. Michalska, *Anal. Chem.*, 2021, **93**, 14737–14742.
10 R. Wang, X. Du, X. Ma, J. Zhai and X. Xie, *Analyst*, 2020, **145**, 3846–3850.
11 W. Yang, J. Zhai and X. Xie, *Analyst*, 2019, **144**, 5617–5623.
12 J. Zhai, D. Yuan and X. Xie, *Sens. Diagn.*, 2022, **1**, 213–221.
13 E. Zdrachek and E. Bakker, *Acc. Chem. Res.*, 2019, **52**, 1400–1408.
14 X. Du, N. Li, Q. Chen, Z. Wu, J. Zhai and X. Xie, *Biomicrofluidics*, 2022, **16**, 031301.
15 R. Sitko, P. Janik, B. Feist, E. Talik and A. Gagor, *ACS Appl. Mater. Interfaces*, 2014, **6**, 20144–20153.
16 G. M. Hieftje, *J. Chem. Educ.*, 2000, **77**, 577–583.
17 M. Fredrikson, N. G. Carlsson, A. Almgren and A. S. Sandberg, *J. Agric. Food Chem.*, 2002, **50**, 59–65.
18 G. F. d. S. Neto, M. L. d. A. Rodrigues and A. Fonseca, *Talanta*, 2021, **221**, 121602.

19 B. Meermann and V. Nischwitz, *J. Anal. At. Spectrom.*, 2018, **33**, 1432–1468.
20 G. Dimeski, T. Badrick and A. S. John, *Clin. Chim. Acta*, 2010, **411**, 309–317.
21 J. Koryta, *Annu. Rev. Mater. Sci.*, 1986, **16**, 13–27.
22 S. Jansod and E. Bakker, *ACS Sens.*, 2019, **4**, 1008–1016.
23 T. Han, U. Vanamo and J. Bobacka, *ChemElectroChem*, 2016, **3**, 2071–2077.
24 M. Urbanowicz, D. G. Pijanowska, A. Jasiński, M. Ekman and M. K. Bocheńska, *J. Solid State Electrochem.*, 2019, **23**, 3299–3308.
25 B. Hambly, M. Guzinski, B. Pendley and E. Lindner, *ACS Sens.*, 2020, **5**, 2146–2154.
26 K. Yu, N. He, N. Kumar, N. X. Wang, J. Bobacka and A. Ivaska, *Electrochim. Acta*, 2017, **228**, 66–75.
27 R. Liang, T. Yin and W. Qin, *Anal. Chim. Acta*, 2015, **853**, 291–296.
28 T. Han, U. Mattinen and J. Bobacka, *ACS Sens.*, 2019, **4**, 900–906.
29 V. Kumar, R. Suri and S. Mittal, *J. Iran. Chem. Soc.*, 2023, **20**, 509–540.
30 T. N. T. Tran, S. Qiu and H. Chung, *IEEE Sens. J.*, 2018, **18**, 9081–9087.
31 J. Bobacka, A. Ivaska and A. Lewenstam, *Chem. Rev.*, 2008, **108**, 329–351.
32 J. Bobacka, *Electroanalysis*, 2006, **18**, 7–18.
33 E. Lindner and R. E. Gyurcsányi, *J. Solid State Electrochem.*, 2009, **13**, 51–68.
34 J. Kozma, S. Papp and R. E. Gyurcsányi, *Bioelectrochemistry*, 2023, **150**, 108352.
35 R. W. Burnett, A. K. Covington, N. Fogh-Andersen, W. R. Külpmann, A. Lewenstam, A. H. J. Maas, O. Müller-Plathe, A. L. Vankessel and W. G. Zijlstra, *Clin. Chem. Lab. Med.*, 2000, **38**, 363–370.
36 D. P. Quan, L. T. Duan, C. X. Quang and P. H. Viet, *Anal. Sci.*, 2001, **17**, 749–752.
37 J. Zhu, Y. Qin and Y. Zhang, *Electrochem. Commun.*, 2009, **11**, 1684–1687.
38 C. Ocaña, M. Muñoz-Correas, N. Abramova and A. Bratov, *Sensors*, 2020, **20**, 1–12.
39 H. Hisamoto and K. Suzuki, *TrAC, Trends Anal. Chem.*, 1999, **18**, 513–524.
40 X. Xie and E. Bakker, *Anal. Bioanal. Chem.*, 2015, **407**, 3899–3910.
41 E. Bakker, P. Bühlmann and E. Pretsch, *Chem. Rev.*, 1997, **97**, 3083–3132.
42 H. Shibata, T. G. Henares, K. Yamada, K. Suzuki and D. Citterio, *Analyst*, 2018, **143**, 678–686.
43 K. N. Mikhelson and M. A. Peshkova, *Russ. Chem. Rev.*, 2015, **84**, 555–578.
44 K. Koren and S. E. Zieger, *ACS Sens.*, 2021, **6**, 1671–1680.
45 J. Migdilski, T. Blaz and A. Lewenstam, *Anal. Chim. Acta*, 1996, **322**, 141–149.
46 M. Gicevičius, A. Ramanavičiene, L. Mikoliunaite and A. Ramanavičius, *2017 IEEE 7th Int. Conf. Nanomater. Appl. Prop. (NAP), Odessa, Ukr.*, 2017, 04NB29-1-04NB29-3.
47 Y. Wang, A. Liu, Y. Han and T. Li, *Polym. Int.*, 2020, **69**, 7–17.
48 M. H. Naveen, N. G. Gurudatt and Y. B. Shim, *Appl. Mater. Today*, 2017, **9**, 419–433.
49 R. Ansari, A. F. Delavar and A. Mohammad-Khah, *J. Solid State Electrochem.*, 2012, **16**, 3315–3322.
50 G. Anantha-Iyengar, K. Shanmugasundaram, M. Nallal, K. P. Lee, M. J. Whitcombe, D. Lakshmi and G. Sai-Anand, *Prog. Polym. Sci.*, 2019, **88**, 1–129.
51 Z. A. Boeva and T. Lindfors, *Sens. Actuators, B*, 2015, **224**, 624–631.
52 C. Wardak, K. Pietrzak, K. Morawska and M. Grabarczyk, *Sensors*, 2023, **23**, 5839.
53 K. Pietrzak, C. Wardak and S. Malinowski, *Appl. Nanosci.*, 2021, **11**, 2823–2835.
54 J. Bobacka, M. McCarrick, A. Lewenstam and A. Ivaska, *Analyst*, 1994, **119**, 1985–1991.
55 C. He, G. Li, Y. Wang and W. Zhou, *Int. J. Electrochem. Sci.*, 2020, **15**, 8096–8107.
56 L. Zhang, Z. Wei and P. Liu, *PLoS One*, 2020, **15**, 1–14.
57 V. K. Gupta, D. K. Chauhan, V. K. Saini, S. Agarwal, M. M. Antonijevic and H. Lang, *Sensors*, 2003, **3**, 223–235.
58 C. M. A. Brett and A. M. Oliveira-Brett, *J. Solid State Electrochem.*, 2011, **15**, 1487–1494.
59 E. Desimoni and I. Bassani, *Anal. Commun.*, 1999, **36**, 45–46.
60 M. Odijk, E. J. Van Der Wouden, W. Olthuis, M. D. Ferrari, E. A. Tolner, A. M. J. M. Van Den Maagdenberg and A. Van Den Berg, *Sens. Actuators, B*, 2015, **207**, 945–953.
61 J. Bobacka, T. Lindfors, M. McCarrick, A. Ivaska and A. Lewenstam, *Anal. Chem.*, 1995, **67**, 3819–3823.
62 A. Michalska, *Electroanalysis*, 2012, **24**, 1253–1265.
63 S. Anastasova-Ivanova, U. Mattinen, A. Radu, J. Bobacka, A. Lewenstam, J. Migdalski, M. Danielewski and D. Diamond, *Sens. Actuators, B*, 2010, **146**, 199–205.
64 R. W. Cattrall and H. Freiser, *Anal. Chem.*, 1971, **43**, 1905–1906.
65 J. Kim, D. H. Kim, J. C. Yang, J. S. Kim, J. H. Lee and S. H. Jung, *Sensors*, 2020, **20**, 1–8.
66 Z. Mousavi, J. Bobacka, A. Lewenstam and A. Ivaska, *J. Electroanal. Chem.*, 2009, **633**, 246–252.
67 R. E. Gyurcsányi, A. S. Nybäck, K. Tóth, G. Nagy and A. Ivaska, *Analyst*, 1998, **123**, 1339–1344.
68 J. Kozma, S. Papp and R. E. Gyurcsányi, *Anal. Chem.*, 2022, **94**, 8249–8257.
69 F. Faridbod, M. R. Ganjali, R. Dinarvand and P. Norouzi, *Sensors*, 2008, **8**, 2331–2412.
70 T. F. Otero and E. de Larreta-Azelain, *Polymer*, 1988, **29**, 1522–1527.
71 M. Watanabe, H. Shirai and T. Hirai, *J. Appl. Phys.*, 2002, **92**, 4631–4637.
72 H. Bao, J. Ye, X. Zhao and Y. Zhang, *Molecules*, 2023, **28**, 1–10.
73 M. Vázquez, P. Danielsson, J. Bobacka, A. Lewenstam and A. Ivaska, *Sens. Actuators, B*, 2004, **97**, 182–189.
74 T. Lindfors, *J. Solid State Electrochem.*, 2009, **13**, 77–89.
75 Z. Pławińska, A. Michalska and K. Maksymiuk, *Electrochim. Acta*, 2016, **187**, 397–405.
76 K. Pietrzak, K. Morawska, S. Malinowski and C. Wardak, *Membranes*, 2022, **12**, 1150.

77 J. Bobacka, A. Ivaska and A. Lewenstam, *Electroanalysis*, 2003, **15**, 366–374.
78 U. Vanamo, E. Hupa, V. Yrjänä and J. Bobacka, *Anal. Chem.*, 2016, **88**, 4369–4374.
79 A. Shvarev, B. Neel and E. Bakker, *Anal. Chem.*, 2012, **84**, 8038–8044.
80 S. Thomas, J. Izquierdo, N. Birbilis and R. M. Souto, *Corrosion*, 2015, **71**, 171–183.
81 Y. Lyu, S. Gan, Y. Bao, L. Zhong, J. Xu, W. Wang, Z. Liu, Y. Ma, G. Yang and L. Niu, *Membranes*, 2020, **10**, 1–24.
82 E. A. Jaramillo and A. C. Noell, *Electroanalysis*, 2020, **32**, 1896–1904.
83 M. Fibbioli, W. E. Morf, M. Badertscher, N. F. De Rooij and E. Pretsch, *Electroanalysis*, 2000, **12**, 1286–1292.
84 J. Hu, A. Stein and P. Bühlmann, *TrAC, Trends Anal. Chem.*, 2016, **76**, 102–114.
85 E. Zdrachek and E. Bakker, *Anal. Chem.*, 2018, **90**, 7591–7599.
86 N. Lenar, R. Piech and B. Paczosa-Bator, *Membranes*, 2022, **12**, 349.
87 D. Y. Imali, E. C. J. Perera, M. N. Kaumal and D. P. Dissanayake, *RSC Adv.*, 2023, **13**, 6396–6411.
88 G. Batrinescu, L. A. Constantin, A. Cuciureanu and M. A. Constantin, in *Conducting Polymers*, 2016, pp. 1–26.
89 J. Sutter and E. Pretsch, *Electroanalysis*, 2006, **18**, 19–25.
90 A. Michalska, A. Konopka and M. Maj-Zurawska, *Anal. Chem.*, 2003, **75**, 141–144.
91 N. He, S. Papp, T. Lindfors, L. Höfler, R. M. Latonen and R. E. Gyurcsányi, *Anal. Chem.*, 2017, **89**, 2598–2605.
92 J. Bobacka, *Anal. Chem.*, 1999, **71**, 4932–4937.
93 C. R. Rousseau and P. Bühlmann, *TrAC, Trends Anal. Chem.*, 2021, **140**, 116277.
94 Z. Mousavi, A. Teter, A. Lewenstam, M. Maj-Zurawska, A. Ivaska and J. Bobacka, *Electroanalysis*, 2011, **23**, 1352–1358.
95 A. Michalska, J. Dumańska and K. Maksymiuk, *Anal. Chem.*, 2003, **75**, 4964–4974.
96 J. Sutter, A. Radu, S. Peper, E. Bakker and E. Pretsch, *Anal. Chim. Acta*, 2004, **523**, 53–59.
97 T. Lindfors, J. Bobacka, A. Lewenstam and A. Ivaska, *Analyst*, 1996, **121**, 1823–1827.
98 E. Pretsch, *TrAC, Trends Anal. Chem.*, 2007, **26**, 46–51.
99 J. Sutter, E. Lindner, R. E. Gyurcsányi and E. Pretsch, *Anal. Bioanal. Chem.*, 2004, **380**, 7–14.
100 M. Guziński, G. Lisak, T. Sokalski, J. Bobacka, A. Ivaska, M. Bocheńska and A. Lewenstam, *Anal. Chem.*, 2013, **85**, 1555–1561.
101 A. Konopka, T. Sokalski, A. Michalska, A. Lewenstam and M. Maj-Zurawska, *Anal. Chem.*, 2004, **76**, 6410–6418.
102 K. Y. Chumbimuni-Torres, N. Rubinova, A. Radu, L. T. Kubota and E. Bakker, *Anal. Chem.*, 2006, **78**, 1318–1322.
103 T. Lindfors and A. Ivaska, *Anal. Chem.*, 2004, **76**, 4387–4394.
104 A. Cadogan, Z. Gao, A. Lewenstam, A. Ivaska, D. Diamond, A. Lewenstam and Z. Gao, *Anal. Chem.*, 1992, **64**, 2496–2501.
105 X. U. Zou, X. V. Zhen, J. H. Cheong and P. Bühlmann, *Anal. Chem.*, 2014, **86**, 8687–8692.
106 U. Vanamo and J. Bobacka, *Electrochim. Acta*, 2014, **122**, 316–321.
107 U. Vanamo and J. Bobacka, *Anal. Chem.*, 2014, **86**, 10540–10545.
108 C. Z. Lai, M. A. Fierke, A. Stein and P. Bühlmann, *Anal. Chem.*, 2007, **79**, 4621–4626.
109 J. P. Veder, R. De Marco, G. Clarke, R. Chester, A. Nelson, K. Prince, E. Pretsch and E. Bakker, *Anal. Chem.*, 2008, **80**, 6731–6740.
110 R. De Marco, J. P. Veder, G. Clarke, A. Nelson, K. Prince, E. Pretsch and E. Bakker, *Phys. Chem. Chem. Phys.*, 2008, **10**, 73–76.
111 H. Liu, Z. Gu, Q. Zhao, S. Li, X. Ding, X. Xiao and G. Xiu, *Sens. Actuators, B*, 2022, **355**, 131102.
112 D. Diamond, *Anal. Chem.*, 2004, **76**, 278A–286A.
113 E. Bakker, V. Bhakthavatsalam and K. L. Gemene, *Talanta*, 2008, **75**, 629–635.
114 K. N. Mikhelson and M. A. Peshkova, *Russ. Chem. Rev.*, 2015, **84**, 555–578.
115 M. A. Peshkova, T. Sokalski, K. N. Mikhelson and A. Lewenstam, *Anal. Chem.*, 2008, **80**, 9181–9187.
116 E. Jaworska, M. Mazur, K. Maksymiuk and A. Michalska, *Anal. Chem.*, 2018, **90**, 2625–2630.
117 S. Papp, M. Bojtár, R. E. Gyurcsányi and T. Lindfors, *Anal. Chem.*, 2019, **91**, 9111–9118.
118 F. Garnier, *Adv. Mater.*, 1989, **1**, 117–121.
119 S. Wang, Y. Kang, L. Wang, H. Zhang, Y. Wang and Y. Wang, *Sens. Actuators, B*, 2013, **182**, 467–481.
120 A. Abbaspour, J. Tashkhourian, S. Ahmadpour, E. Mirahmadi, H. Sharghi, R. Khalifeh and M. R. Shahriyari, *Mater. Sci. Eng., C*, 2014, **34**, 326–333.
121 B. Liu, X. Zhao, Y. Xiao and M. Cao, *J. Mater. Chem. A*, 2014, **2**, 3338–3343.
122 W. Wang, G. Xu, X. T. Cui, G. Sheng and X. Luo, *Biosens. Bioelectron.*, 2014, **58**, 153–156.
123 A. M. Mahmoud, M. K. Abd El-Rahman, M. R. Elghobashy and M. R. Rezk, *J. Electroanal. Chem.*, 2015, **755**, 122–126.
124 L. Tian, J. Qiu, Y. C. Zhou and S. G. Sun, *Microchim. Acta*, 2010, **169**, 269–275.
125 J. Schwarz, K. Trommer and M. Mertig, *Am. J. Anal. Chem.*, 2018, **9**, 591–601.
126 M. R. Tamara, D. Lelono, R. Roto and K. Triyana, *Sens. Actuators, A*, 2023, **351**, 114170.
127 I. Ivanko, T. Lindfors, R. Emanuelsson and M. Sjödin, *Sens. Actuators, B*, 2021, **329**, 1–9.
128 D. Lakshmi, M. J. Whitcombe, F. Davis, I. Chianella, E. V. Piletska, A. Guerreiro, S. Subrahmanyam, P. S. Brito, S. A. Fowler and S. A. Piletsky, *Chem. Commun.*, 2009, 2759–2761.
129 S. Wang, B. Liu, Z. Duan, Q. Zhao, Y. Zhang, G. Xie, Y. Jiang, S. Li and H. Tai, *Sens. Actuators, B*, 2021, **327**, 128923.
130 B. Liu, Z. Duan, Z. Yuan, Y. Zhang, Q. Zhao, G. Xie, Y. Jiang, S. Li and H. Tai, *ACS Appl. Mater. Interfaces*, 2022, **14**, 27203–27213.

131 S. Wang, Y. Jiang, B. Liu, Z. Duan, H. Pan, Z. Yuan, G. Xie, J. Wang, Z. Fang and H. Tai, *Sens. Actuators, B*, 2021, **343**, 130069.
132 C. Liu, X. Jiang, Y. Zhao, W. Jiang, Z. Zhang and L. Yu, *Electrochim. Acta*, 2017, **231**, 53–60.
133 N. Abramova, J. Moral-Vico, J. Soley, C. Ocaña and A. Bratov, *Anal. Chim. Acta*, 2016, **943**, 50–57.
134 W. Jiang, C. Liu, Y. Zhao, G. I. N. Waterhouse, Z. Zhang and L. Yu, *Synth. Met.*, 2019, **248**, 94–101.
135 X. Zeng, W. Jiang, X. Jiang, G. I. N. Waterhouse, Z. Zhang and L. Yu, *Anal. Chim. Acta*, 2020, **1094**, 26–33.
136 X. Zeng, W. Jiang, G. I. N. Waterhouse, X. Jiang, Z. Zhang and L. Yu, *Microchim. Acta*, 2021, **188**, 393.
137 A. K. R. Police, M. Chennaiahgari, R. Boddula, S. V. P. Vattikuti, K. K. Mandari and B. Chan, *Mater. Res. Bull.*, 2018, **98**, 314–321.
138 A. Ramadoss and S. J. Kim, *Carbon*, 2013, **63**, 434–445.
139 H. Su, T. Wang, S. Zhang, J. Song, C. Mao, H. Niu, B. Jin, J. Wu and Y. Tian, *Solid State Sci.*, 2012, **14**, 677–681.
140 J. Wu, X. Chen, Q. Wang, Y. Bian, K. Zhang, Z. Sheng, J. Jin, M. Yang, P. Dai, X. Fu, W. Chang and C. Xie, *Electroanalysis*, 2018, **30**, 1812–1819.
141 V. D. Yadav, R. Jain and P. Dandekar, *Mater. Res. Express*, 2017, **4**, 085015.
142 J. Sophia and G. Muralidharan, *Sens. Actuators, B*, 2014, **193**, 149–156.
143 X. Fan, P. Lin, S. Liang, N. Hui, R. Zhang, J. Feng and G. Xu, *Ionics*, 2017, **23**, 997–1003.
144 G. Cepriá, J. Pardo, A. Lopez, E. Peña and J. R. Castillo, *Sens. Actuators, B*, 2016, **230**, 25–30.
145 H. Wang, Q. Hao, X. Yang, L. Lu and X. Wang, *Nanoscale*, 2010, **2**, 2164–2170.
146 M. Rutkowska, T. Lindfors, Z. Boeva and M. Strawski, *Sens. Actuators, B*, 2021, **337**, 129808.
147 T. Lindfors and A. Ivaska, *J. Electroanal. Chem.*, 2002, **531**, 43–52.
148 Y. Bao, J. Yan, J. Hu and J. Li, *Sens. Actuators, B*, 2023, **390**, 133997.
149 N. A. Abdallah, S. A. Ahmed, M. Almaghrabi and Y. M. Alahmadi, *Polymers*, 2023, **15**, 3991.
150 G. Xu, S. Liang, J. Fan, G. Sheng and X. Luo, *Microchim. Acta*, 2016, **183**, 2031–2037.
151 Y. Wang, H. Xu, X. Yang, Z. Luo, J. Zhang and G. Li, *Sens. Actuators, B*, 2012, **173**, 630–635.
152 E. Hupa, U. Vanamo and J. Bobacka, *Electroanalysis*, 2015, **27**, 591–594.
153 N. Lenar, R. Piech and B. Paczosa-Bator, *Materials*, 2021, **14**, 1891.
154 C. Bahro, S. Goswami, S. Gernhart and D. Koley, *Anal. Chem.*, 2022, **94**, 8302–8308.
155 M. Guzinski, J. M. Jarvis, F. Perez, B. D. Pendley, E. Lindner, R. De Marco, G. A. Crespo, R. G. Acres, R. Walker and J. Bishop, *Anal. Chem.*, 2017, **89**, 3508–3516.
156 Z. H. Neo, G. E. K. K. Seah, S. H. Ng, D. Safanama, D. H. L. Seng and S. S. Goh, *Anal. Chem.*, 2022, **94**, 15956–15963.
157 M. Guzinski, J. M. Jarvis, P. D'Orazio, A. Izadyar, B. D. Pendley and E. Lindner, *Anal. Chem.*, 2017, **89**, 8468–8475.
158 J. Szucs, T. Lindfors, J. Bobacka and R. E. Gyurcsányi, *Electroanalysis*, 2016, **28**, 778–786.
159 X. Luo, C. L. Weaver, D. D. Zhou, R. Greenberg and X. T. Cui, *Biomaterials*, 2011, **32**, 5551–5557.
160 A. J. Bandodkar, I. Jeerapan and J. Wang, *ACS Sens.*, 2016, **1**, 464–482.
161 W. Gao, S. Emaminejad, H. Y. Y. Nyein, S. Challa, K. Chen, A. Peck, H. M. Fahad, H. Ota, H. Shiraki, D. Kiriya, D. H. Lien, G. A. Brooks, R. W. Davis and A. Javey, *Nature*, 2016, **529**, 509–514.
162 M. D. Steinberg, P. Kassal and I. M. Steinberg, *Electroanalysis*, 2016, **28**, 1149–1169.
163 N. Tang, Y. Zheng, H. Haick, X. Jiang, C. Zhou, H. Jin, K. Jin and W. Wu, *Micromachines*, 2021, **12**, 1–15.
164 A. Michalska, *Anal. Bioanal. Chem.*, 2006, **384**, 391–406.
165 N. Lenar, B. Paczosa-Bator, R. Piech and A. Królicka, *Electrochim. Acta*, 2019, **322**, 134718.
166 M. A. Ali, X. Wang, Y. Chen, Y. Jiao, N. K. Mahal, S. Moru, M. J. Castellano, J. C. Schnable, P. S. Schnable and L. Dong, *ACS Appl. Mater. Interfaces*, 2019, **11**, 29195–29206.
167 N. Lenar, B. Paczosa-Bator and R. Piech, *Microchim. Acta*, 2019, **186**, 777.
168 J. M. Jarvis, M. Guzinski, B. D. Pendley and E. Lindner, *J. Solid State Electrochem.*, 2016, **20**, 3033–3041.
169 D. Kałuża, E. Jaworska, M. Mazur, K. Maksymiuk and A. Michalska, *Anal. Chem.*, 2019, **91**, 9010–9017.
170 N. Lenar, R. Piech and B. Paczosa-Bator, *J. Electrochem. Soc.*, 2022, **169**, 127508.
171 A. V. Bondar, V. M. Keresten and K. N. Mikhelson, *J. Anal. Chem.*, 2022, **77**, 145–154.
172 A. Lewenstam, *Electroanalysis*, 2014, **26**, 1171–1181.
173 E. Zdrachek and E. Bakker, *Anal. Chem.*, 2021, **93**, 72–102.
174 K. Maksymiuk, E. Stelmach and A. Michalska, *Membranes*, 2020, **10**, 1–15.
175 K. Węgrzyn, J. Kalisz, E. Stelmach, K. Maksymiuk and A. Michalska, *Anal. Chem.*, 2021, **93**, 10084–10089.
176 E. Bakker, *TrAC, Trends Anal. Chem.*, 2014, **53**, 98–105.
177 M. Mir, R. Lugo, I. B. Tahirbegi and J. Samitier, *Sensors*, 2014, **14**, 11844–11854.
178 A. J. Bandodkar and J. Wang, *Trends Biotechnol.*, 2014, **32**, 363–371.
179 C. Zuliani and D. Diamond, *Electrochim. Acta*, 2012, **84**, 29–34.
180 T. Han, A. V. Kalinichev, Z. Mousavi, K. N. Mikhelson and J. Bobacka, *Sens. Actuators, B*, 2022, **357**, 131416.
181 A. Michalska, M. Wojciechowski, B. Wagner, E. Bulska and K. Maksymiuk, *Anal. Chem.*, 2006, **78**, 5584–5589.
182 L. Y. Heng, K. Toth and E. A. H. Hall, *Talanta*, 2004, **63**, 73–87.
183 A. Michalska, M. Wojciechowski, E. Bulska, J. Mieczkowski and K. Maksymiuk, *Talanta*, 2009, **79**, 1247–1251.
184 E. Woźnica, J. Mieczkowski and A. Michalska, *Analyst*, 2011, **136**, 4787–4793.

185 E. Jaworska, A. Kisiel, K. Maksymiuk and A. Michalska, *Anal. Chem.*, 2011, **83**, 438–445.
186 U. Fiedler and J. Růžička, *Anal. Chim. Acta*, 1973, **67**, 179–193.
187 P. Itterheimová, J. Bobacka, V. Šindelář and P. Lubal, *Chemosensors*, 2022, **10**, 1–16.
188 J. Bobacka, Z. Gao, A. Ivaska and A. Lewenstam, *J. Electroanal. Chem.*, 1994, **368**, 33–41.
189 R. Qian, Q. Pei and Y. Li, *Synth. Met.*, 1993, **61**, 275–278.
190 A. Michalska and K. Maksymiuk, *Electrochim. Acta*, 1999, **44**, 2125–2129.
191 A. Michalska and A. Lewenstam, *Anal. Chim. Acta*, 2000, **406**, 159–169.
192 E. Jaworska, K. Maksymiuk and A. Michalska, *Electroanalysis*, 2023, **35**, 1–7.
193 G. Zotti, *Synth. Met.*, 1992, **51**, 373–382.
194 R. Ansari Khalkhali, W. E. Price and G. G. Wallace, *React. Funct. Polym.*, 2003, **56**, 141–146.
195 G. G. Wallace, P. R. Teasdale, G. M. Spinks and L. A. P. Kane-Maguire, *Conductive Electroactive Polymers, Intelligent Materials Systems*, Boca Raton, 2nd edn, 2002.
196 L. X. Wang, X. G. Li and Y. L. Yang, *React. Funct. Polym.*, 2001, **47**, 125–139.
197 W. Gao, W. Jing, Y. Du, Z. Li, P. Liu, F. Han, L. Zhao, Z. Yang and Z. Jiang, *Micromachines*, 2023, **14**, 855.
198 E. Stelmach, B. Kaczmarczyk, K. Maksymiuk and A. Michalska, *Talanta*, 2020, **211**, 120663.
199 P. Kraikaew, Y. Soda, R. Nussbaum, S. Jeanneret and E. Bakker, *Sens. Actuators, B*, 2023, **379**, 133220.
200 E. Grygolowicz-Pawlak and E. Bakker, *Anal. Chem.*, 2010, **82**, 4537–4542.
201 H. J. Lee, I. J. Yoon, C. L. Yoo, H. J. Pyun, G. S. Cha and H. Nam, *Anal. Chem.*, 2000, **72**, 4694–4699.
202 K. Cammann and G. A. Rechnitz, *Anal. Chem.*, 1976, **48**, 856–862.
203 K. N. Mikhelson, J. Bobacka, A. Ivaska, A. Lewenstam and M. Bochenska, *Anal. Chem.*, 2002, **74**, 518–527.
204 M. A. Peshkova, E. S. Koltashova, G. A. Khripoun and K. N. Mikhelson, *Electrochim. Acta*, 2015, **167**, 187–193.
205 Y. Mi, S. Mathison and E. Bakker, *Electrochem. Solid-State Lett.*, 1999, **2**, 198–200.
206 A. Shvarev and E. Bakker, *J. Am. Chem. Soc.*, 2003, **125**, 11192–11193.
207 K. L. Gemene, A. Shvarev and E. Bakker, *Anal. Chim. Acta*, 2007, **583**, 190–196.
208 Y. Kim and S. Amemiya, *Anal. Chem.*, 2008, **80**, 6056–6065.
209 E. Jaworska, A. Kisiel, K. Maksymiuk and A. Michalska, *Anal. Chem.*, 2011, **83**, 438–445.
210 X. Xie, I. Szilagyi, J. Zhai, L. Wang and E. Bakker, *ACS Sens.*, 2016, **1**, 516–520.
211 K. J. Robinson, Y. Soda and E. Bakker, *Chem. Commun.*, 2022, **58**, 4279–4287.
212 J. Lee, Y. K. Hahn, J. Y. Park, H. Seo, J. Jung, E. Cho, Y. S. Choi and S. S. Lee, *Sens. Actuators, B*, 2019, **280**, 256–262.
213 A. Konefał, P. Piątek, K. Maksymiuk and A. Michalska, *Sens. Actuators, B*, 2023, **391**, 134022.
214 H. He, H. Li, G. Mohr, B. Kovacs, T. Werner and O. S. Wolfbeis, *Anal. Chem.*, 1993, **65**, 123–127.
215 A. Kisiel, B. Baniak, K. Maksymiuk and A. Michalska, *Talanta*, 2020, **220**, 121358.
216 M. Shortreed, E. Bakker and R. Kopelman, *Anal. Chem.*, 1996, **68**, 2656–2662.
217 H. Hisamoto, N. Miyashita, K. Watanabe, E. Nakagawa, N. Yamamoto and K. Suzuki, *Sens. Actuators, B*, 1995, **29**, 378–385.
218 X. Xie, X. Li, Y. Ge, Y. Qin and H. Y. Chen, *Sens. Actuators, B*, 2010, **151**, 71–76.
219 M. T. Bamsey, A. Berinstain and M. A. Dixon, *Sens. Actuators, B*, 2014, **190**, 61–69.
220 A. Kisiel, K. Maksymiuk and A. Michalska, *Sens. Actuators, B*, 2018, **273**, 1730–1734.
221 X. Xie, G. Mistlberger and E. Bakker, *Anal. Chem.*, 2013, **85**, 9932–9938.
222 K. Kłucińska, E. Stelmach, A. Kisiel, K. Maksymiuk and A. Michalska, *Anal. Chem.*, 2016, **88**, 5644–5648.
223 H. A. Clark, M. Hoyer, M. A. Philbert and R. Kopelman, *Anal. Chem.*, 1999, **71**, 4831–4836.
224 A. Kisiel, K. Kłucińska, Z. Głębicka, M. Gniadek, K. Maksymiuk and A. Michalska, *Analyst*, 2014, **139**, 2515–2524.
225 X. Wang, Q. Zhang, C. Nam, M. Hickner, M. Mahoney and M. E. Meyerhoff, *Angew. Chem., Int. Ed.*, 2017, **56**, 11826–11830.
226 X. Du and X. Xie, *Sens. Actuators, B*, 2021, **335**, 129368.
227 X. Xie, *Anal. Bioanal. Chem.*, 2016, **408**, 2717–2725.
228 R. Wang and X. Wang, *Sens. Actuators, B*, 2021, **329**, 129171.
229 W. E. Morf, K. Seiler, B. Rusterholz and W. Simon, *Anal. Chem.*, 1990, **62**, 738–742.
230 R. Narayanaswamy, *Biosens. Bioelectron.*, 1991, **6**, 467–475.
231 T. Sokalski, T. Zwickl, E. Bakker and E. Pretsch, *Anal. Chem.*, 1999, **71**, 1204–1209.
232 M. J. Ruedas-Rama and E. A. H. Hall, *Analyst*, 2006, **131**, 1282–1291.
233 J. Langmaier and E. Lindner, *Anal. Chim. Acta*, 2005, **543**, 156–166.
234 E. Stelmach, K. Kłucińska, K. Maksymiuk and A. Michalska, *Talanta*, 2019, **196**, 226–230.
235 L. Wang, X. Xie, T. Cao, J. Bosset and E. Bakker, *Chem.–Eur. J.*, 2018, **24**, 7921–7925.
236 T. Danno, K. Kobayashi and A. Tanioka, *J. Appl. Polym. Sci.*, 2006, **100**, 3111–3115.
237 W. Wang, J. Lin, C. Cai and S. Lin, *Eur. Polym. J.*, 2015, **65**, 112–131.
238 A. Konefał, P. Piątek, B. Paterczyk, K. Maksymiuk and A. Michalska, *Talanta*, 2023, **253**, 124038.
239 E. Woźnica, K. Maksymiuk and A. Michalska, *Anal. Chem.*, 2014, **86**, 411–418.
240 R. Traiphol, P. Sanguansat, T. Srikhirin, T. Kerdcharoen and T. Osotchan, *Macromolecules*, 2006, **39**, 1165–1172.